ELSEVIER

Marine Geology 210 (2004) 79–105

MARINE GEOLOGY
INTERNATIONAL JOURNAL OF MARINE GEOLOGY, GEOCHEMISTRY AND GEOPHYSICS

www.elsevier.com/locate/margeo

The generation and preservation of multiple hurricane beds in the northern Gulf of Mexico

Timothy R. Keen[a,*], Samuel J. Bentley[b], W. Chad Vaughan[c], Cheryl Ann Blain[a]

[a] *Naval Research Laboratory, Oceanography Division, Stennis Space Center, MS 39529, USA*
[b] *Department of Oceanography and Coastal Sciences and Coastal Studies Institute, Louisiana State University, Baton Rouge, LA 70803, USA*
[c] *Naval Research Laboratory, Seafloor Sciences Division, Stennis Space Center, MS 39529, USA*

Received 20 June 2002; received in revised form 22 February 2003; accepted 3 May 2004

Abstract

Cores collected from Mississippi Sound and the inner shelf of the northeast Gulf of Mexico have been examined using ^{210}Pb and ^{137}Cs geochronology, X-radiography, granulometry, and a multi-sensor core logger. The results indicate that widespread event layers were probably produced by an unnamed hurricane in 1947 and by Hurricane Camille in 1969. Physical and biological post-depositional processes have reworked the event layers, producing regional discontinuities and localized truncation, and resulting in an imperfect and biased record of sedimentary processes during the storms. The oceanographic and sedimentological processes that produced these event beds have been simulated using a suite of numerical models: (1) a parametric cyclone wind model; (2) the SWAN third-generation wave model; (3) the ADCIRC 2D finite-element hydrodynamic model; (4) the Princeton Ocean Model; (5) a coupled wave–current bottom boundary layer-sedimentation model; and (6) a model for bed preservation potential as a function of burial rate and bioturbation rate. Simulated cores from the Mississippi Sound region are consistent with the observed stratigraphy and geochronology on both the landward and seaward sides of the barrier islands.

Keywords: hurricanes; numerical models; event beds; geochronology; Gulf of Mexico

1. Introduction

Ancient continental shelf strata frequently consist of intercalated sand and shale or mudstone beds. A storm origin is inferred for the sand beds when they contain hummocky cross stratification (HCS) and have erosive bases (Dott and Bourgeois, 1982). Storm beds containing HCS range in thickness from about 0.1 to 2 m. It has been suggested that this association of mud (deposited under more quiescent conditions) and sand (storm beds) is deposited in water depths below fair-weather wave base but above storm wave base (Duke, 1985). In contrast to these thick sand layers deposited in deeper water, storm sand beds deposited on the inner shelf and shoreface may comprise less than half the total sediment and be less than 0.1 m thick (Driese et al., 1991). These thinner beds may contain fine-scale HCS and be laterally continuous for less than 10 m.

* Corresponding author. Naval Research Laboratory, Oceanography Division, Stennis Space Center, MS 39529, USA. Tel.: +1-228-828-4950; fax: +1-228-828-4759.
E-mail address: keen@nrlssc.navy.mil (T.R. Keen).

0025-3227/$ - see front matter © 2004 Elsevier B.V. All rights reserved.
doi:10.1016/j.margeo.2004.05.022

Observations from modern continental shelves suggest that storm beds range from 0.01 m on the middle shelf (Hayes, 1967; Morton, 1981; Snedden and Nummedal, 1991) to 0.2 m on the shoreface (Beavers, 1999). Modeling studies also indicate that storm beds are irregular and discontinuous (Keen and Slingerland, 1993a,b; Keen and Glenn, 1998). A remaining problem is the preservation of the storm beds after deposition. In areas where storm beds are amalgamated, it is not possible to identify individual sand layers. However, if significant fine-grained sediment is deposited between intense storms, storm beds may be buried deeply enough to escape reworking. In order to understand the relationship between the initial characteristics of an individual storm bed and its ultimate preservation in the stratigraphic record, it is necessary to examine an event bed that is unique and widely distributed. Bentley et al. (2000, 2002) describe the sand layer deposited by Hurricane Camille in August 1969 near its landfall in an estuary in the northern Gulf of Mexico. Because of the absence of more recent major hurricanes in this region, this event bed has the potential to demonstrate physical and biological influences on the preservation of storm beds.

1.1. Background

The observations needed to evaluate the event layers predicted by single-bed models like that of Keen and Slingerland (1993a) have been scarce in the past because of problems of scale and the preservation of these thin sand beds. Snedden et al. (1988) and Morton (1981) have described the spatial extent of event beds deposited on the Texas coast during hurricanes but definitive evidence of the correlation of these beds was lacking because of reworking of the bed. In order to identify an individual storm bed in multiple cores with sufficient accuracy to test the quantitative predictions of a numerical model, it is necessary to have better control on the time of deposition of possible beds. It is also important that bed amalgamation and reworking are minimal. Because of these difficulties, it has not been possible to simulate multiple event bed deposition at time scales on the order of decades. Longer time scales have been simulated using numerical models (e.g., Thorne et al., 1991).

A category 4 hurricane made landfall on the Louisiana coast north of the modern Balize delta of the Mississippi River on 19 September 1947 (Fig. 1), producing a 4.8-m surge near Bay St. Louis, Mississippi (Neumann, 1993; Stone et al., 1997). Hurricane Camille, which was the second strongest hurricane to hit the U.S. coastline in the 20th century, made landfall on the Mississippi coast (Fig. 1) at 0430 UT on 17 August 1969. The central pressure was 901 mb and the maximum sustained winds near the eye were more than 85 m s^{-1} just before landfall (Anonymous, 1969). The storm surge near landfall within Mississippi Sound exceeded 7 m. Bottom currents on the Florida coast 150 km east of landfall exceeded 1.6 m s^{-1} (Murray, 1970). Prior to Camille, there were no major hurricane strikes along this coast since 1947. Hurricane Georges made landfall near Biloxi, MS, in 1998 (Stone and Wang, 1999). However, Georges was much weaker than Camille, and cores from Mississippi Sound several months after Georges did not contain a significant preserved event layer (Bentley, unpublished data). Thus, Georges is not expected to have had a widespread effect on amalgamation of previous storm beds. It thus seems likely that if multiple identifiable and datable event beds are to be found anywhere in the U.S. coastal waters, it may well be in the sheltered waters of Mississippi Sound.

1.2. Study area

The south-facing barriers islands fronting Mississippi Sound (Fig. 1) formed by upward aggradation as sediment from Mobile Bay was transported westward by longshore currents (Otvos, 1970). Sediment within Mississippi Sound consists of medium to coarse sand along the barrier islands and silt and clay located within the central parts of the sound (Upshaw et al., 1966). Overall, the northern Gulf of Mexico barrier islands are migrating to the west in response to wave-driven longshore drift (Stone and Stapor, 1996). Ship Island, consisting of West Ship Island (WSI) and East Ship Island (ESI), appears to be rotating counterclockwise as East Ship Island is eroding on its Gulf side. The rotation is partly attributed to accretion on the Gulf coast of WSI while erosion is occurring on its sound side.

The Chandeleur Islands are a recurved eastward-facing barrier chain fronting Chandeleur Sound. These islands are migrating west-northwest over the subsiding St. Bernard deltaic plain. Beach deposits consist of shell fragments and fine quartz sand. The sediments of

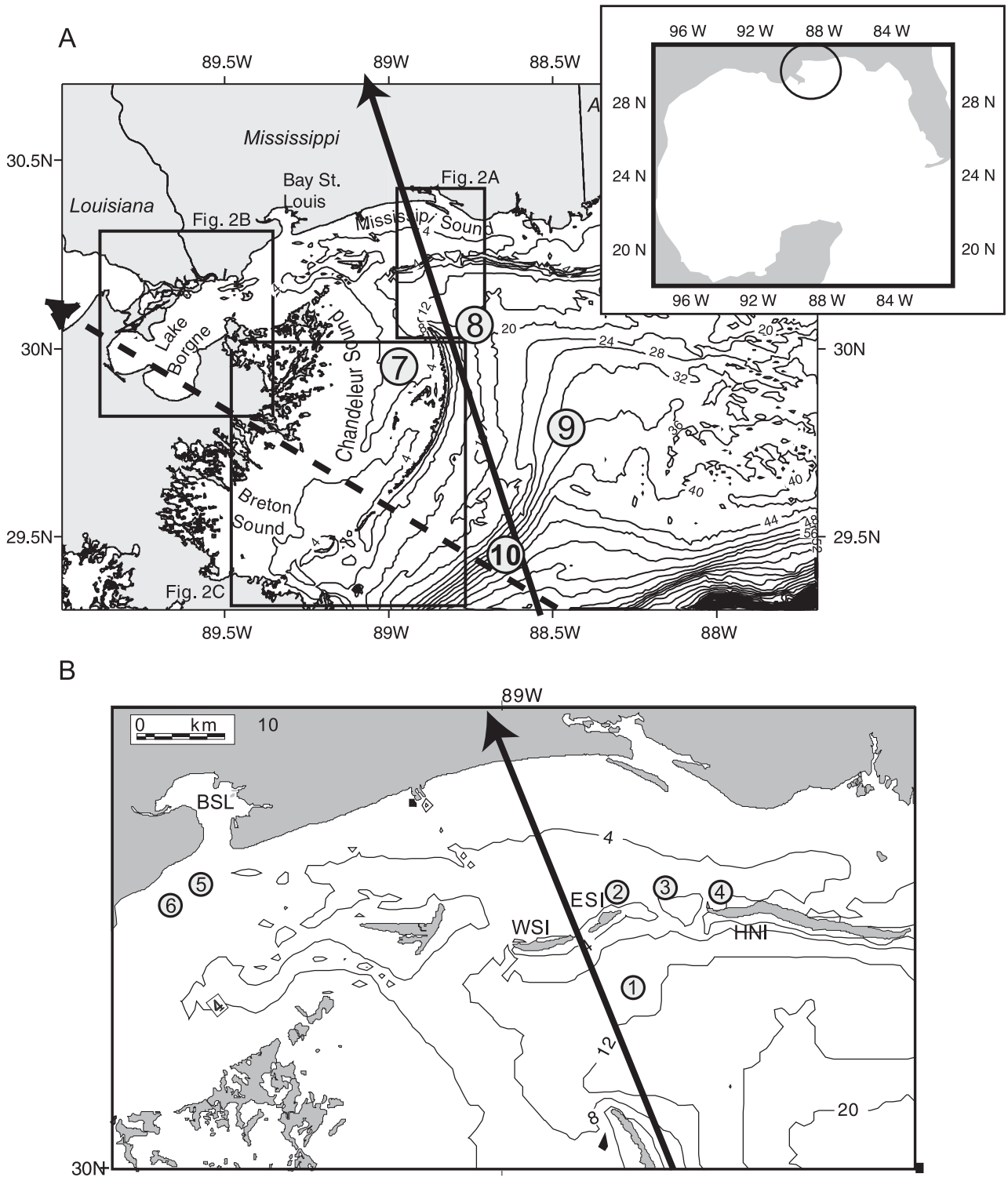

Fig. 1. (A) Map of the Mississippi Bight study area. The boxes refer to sedimentation model subgrids shown in Fig. 2. The 1947 hurricane path is indicated by the dashed line and Hurricane Camille's path is shown by a solid line. (B) Close-up map of the Mississippi Sound area. Key to abbreviations: BSL = Bay St. Louis; WSI = West Ship Island; ESI = East Ship Island; HNI = Horn Island. The core locations listed in Table 1 are shown by circled numbers in panels A and B.

Chandeleur Sound comprise clay, silt and sand. The dominant geomorphic factors in the evolution of the Chandeleur barrier island chain are tropical cyclones, which commonly overwash these low-lying islands (Kahn and Roberts, 1982). However, the established dunes of the northern islands contribute to their durability by directing storm overwash into pre-existing channels. Kahn and Roberts (1982) noted that fair-weather waves and currents rapidly redistributed sediment eroded from the beach and dune system by Hurricane Frederick in 1979. Much of this transported sediment contributes to the longshore drift pool that can rapidly seal storm channels (Nummedal et al., 1980). The beaches of the southern islands are more exposed to storm waves than the northeast-facing beaches of the northern islands. The southern islands are therefore undergoing rapid erosion and northwest migration. Hurricane Frederick flattened the southern Chandeleur Islands, and they remain a shoal today because of more recent storms such as Hurricane Georges in 1998 (Stone and Wang, 1999).

1.3. Objectives

The objectives of this paper are: (1) to use observations and numerical models to constrain the initial extent and thickness of the event beds produced by an unnamed hurricane in 1947 and Hurricane Camille in 1969; and (2) to examine the processes affecting the preservation of the sandy event layers. This paper will show by means of core analysis that the storm beds can be identified in cores from Mississippi Sound and the adjacent shelf. This study also makes quantitative predictions of sediment resuspension and transport within Mississippi Sound and uses them to evaluate patterns of storm bed deposition within the region. Finally, simulated cores that reflect sand and mud storm deposition, fair-weather deposition, and bioturbation are generated for use in discussing the preservation potential of the storm beds.

2. Methods

2.1. Core retrieval and analysis

The Research Vessel *Kit Jones* completed three cruises in the Mississippi bight between July 1999 and July 2000. Box cores and gravity cores (Table 1) were collected in western and central Mississippi Sound and the adjacent inner shelf, in water depths between 4 and 10 m (Fig. 1, Table 1). Additional gravity cores from the middle and outer shelf and Chandeleur Sound (Fig. 1, Table 1) were provided by the Naval Oceanographic Office's Northern Gulf of Mexico Littoral Initiative (NGLI). Inner-shelf sampling stations were located near the mud–sand transition both seaward and landward of the barrier islands, based on the hypothesis that if event layers are preserved, identification would be facilitated by lithologic contrast between sandy event beds and muddy matrix. Box cores were subsampled for radioisotopes and physical properties at 0.01–0.02-m intervals. Slabs taken from the box cores using Plexiglas trays were X-radiographed.

Gravity cores were analyzed using a GEOTEK Multi-Sensor Core Logger (MSCL), an automated system in which cores are logged horizontally. An ultrasonic P-wave system measured P-Wave speed through the cores at 500 kHz. Gamma ray density (attenuation) was measured from a narrow beam of gamma rays emitted from a 10 mCi ^{137}Cs source with energies principally at 661 keV. Measurements were conducted at atmospheric pressure, with cores equil-

Table 1
Summary of core locations and station numbers discussed in this paper

Station number in Fig. 1	Station name	Box cores	Gravity cores
1	Inner Shelf	KJ070600 BC8	KJ070600 GC8
2	East Ship Island	KJ070600 BC6	KJ070600 GC6
3	Dog Keys Pass	KJ040500 E	
4	Horn Island	KJ070600 BC1 KJ040500 D	KJ070600 GC1
5	Bay St. Louis	BSL070999 BCE KJ070999 BCE	BSL091399 GCA
6	Western Mississippi Sound	KJ0501D	KJ0501GCD
7	Chandeleur Sound		1199C3
8	East of Chandeleur Islands		599C2
9	Middle Shelf		599C4
10	Outer Shelf		500C3

ibrated to laboratory ambient temperature (23 °C). Subsamples were retained for radioisotope and granulometric analysis. Patterns of grain size were determined by measuring the percent sand and mud in samples that were dispersed in 0.05% sodium metaphosphate solution, disaggregated in an ultrasonic bath, and wet-sieved using a 4 ϕ (63 μm) screen. The mud and sand fractions were then dried and weighed.

Activities of ^{210}Pb, with a half-life of 22 years, and ^{137}Cs, with a half-life of 30.7 years, were determined by γ-spectroscopic analysis of dried sediment. ^{210}Pb activities were corrected for self-absorption by calibration with standards of known activity (Cutshall et al., 1983). Excess activities of ^{210}Pb (^{210}Pb$_{xs}$) were determined by comparison with supported activities of the parent radionuclides, ^{214}Pb and ^{214}Bi. ^{137}Cs is an anthropogenic impulse tracer that was introduced into the environment in atmospheric atomic bomb testing beginning in 1954. It reached a peak in 1963 and input has been declining ever since. ^{137}Cs usually adsorbs strongly and irreversibly to particle surfaces. The minimum detection limit for ^{137}Cs was 0.05 decays per minute per gram (dpm g^{-1}) in 17-g samples. Activities for all radioisotopes are reported in dpm g^{-1}, with 60 dpm g^{-1} equivalent to 1 Bq g^{-1}.

2.2. Numerical methods

This study uses a linked model system approach similar to that described in Keen and Slingerland (1993a). A parametric wind model is used to generate the hurricane wind fields. The wind fields are used to drive both wave and current models. The predicted current and wave fields are then used to drive a coupled bottom boundary layer-sedimentation model, which predicts resuspension, erosion, and deposition. The bottom topography used in the sedimentation simulations comes from the National Ocean Service (NOS) 3-s database and local surveys made during the NGLI project.

A parametric cyclone wind model, which gives good results for areas within the radius of maximum winds (Keen and Slingerland, 1993a), is used to generate wind fields from available meteorological data. The wind field for these simulations is computed on a 5-km grid of the entire Gulf of Mexico. This study utilizes the third-generation spectral SWAN model (Simulating Waves Nearshore) (Booij et al., 1999; Ris et al., 1999) to compute waves. The SWAN model calculates refraction, diffraction, wave breaking, dissipation, wave–wave interaction, and local wind generation. The water depth used in SWAN changes with the water surface elevation and, therefore, larger storm waves can be computed in otherwise shallow water within the estuary. The elevation comes from the hydrodynamic models. The wave model does not calculate waves over the islands when they are submerged, however. The wave model grid is the same as the wind grid. The storm current fields are computed using different hydrodynamic models as discussed below. The astronomical tides are not calculated for this simulation because of their minimal impact during the hurricane. No river inflow is incorporated into the hydrodynamic models. The circulation models also do not include wetting or drying.

The bottom boundary layer model (BBLM) of Glenn and Grant (1987) has been extended to promote better convergence of the numerical solution for a wider range of wave and current regimes (Keen and Glenn, 1994). This enhanced model is coupled to a sediment transport and bed conservation model. The coupled BBLM-sedimentation model is called TRANS98 (Keen and Glenn, 1998). The sedimentation model uses a grid with a horizontal resolution of approximately 650 m and 31 vertical levels. Wave and current properties must be supplied at each grid point in the domain at each model time step, which is 1 h in this study. The significant wave height H_s, peak period T, and mean propagation direction θ of the wave field are available from the SWAN wave simulation. The wave orbital speed u_b and diameter A_b are computed using linear wave theory. The reference currents u_r are given by depth-integrated currents computed by the hydrodynamic models. The angle φ_r between the current and wave directions is also found. The current and suspended sediment concentration profiles are computed for every time step.

The sediment concentration profiles computed by the BBLM are used to find the depth-integrated suspended sediment transport rate for each size class in suspension:

$$\overrightarrow{S_n} = \int \overrightarrow{u_z} c_{nz} \mathrm{d}z, \tag{1}$$

where $\overrightarrow{u_z}$ is the vector current at height z and c_{nz} is the concentration of size class n at height z. A bed load transport rate is computed from:

$$B_n = \frac{1}{g} A_n c_{bn} (u*_{cw} - u*_n)(\tau_0 - \tau_n), \quad (2)$$

where g is the gravity constant (9.81 m/s^2), A_n is a dynamical parameter with a value of 10, $u*_n$ is the critical shear velocity for grain size n, τ_0 is the maximum shear stress, and τ_n is the critical entrainment shear stress of grain size n. The bed load vector is in the direction of wave propagation. The sediment fluxes found from Eqs. (1) and (2) are used to solve bed conservation equations for the x and y directions. The x-directed conservation equation is given by:

$$\rho_s(1-v)\frac{\partial}{\partial t}(\Delta_y h_n) + \frac{1}{g}\frac{\partial}{\partial x}(\Delta_y B_n) + \frac{\partial S_n}{\partial x} = 0, \quad (3)$$

where ρ_s is the sediment density, v is the bed porosity, h_n is the bed elevation due to size class n. The y direction conservation equation is of similar form.

Since the TRANS98 model as implemented in this study does not include overtopping of barrier islands or coastal areas by the storm surge, it is necessary to represent coastal erosion by introducing sediment at landward grid points. Thus, a no-gradient boundary condition is applied for transports at the coast and at the open boundaries of the model grid. This coastal erosion simulates erosion from the interior of the islands during overwash, as well as beach erosion. Sediment is input to the model grid wherever erosion is predicted at wet points adjacent to land. This boundary condition assumes that landward erosion by waves or overtopping is adequate to supply a sufficient sediment volume to the shallowest wet grid to prevent erosion. This treatment is necessary because the model does not calculate sediment entrainment by breaking waves. A similar boundary condition is included at open boundaries, except that sediment can leave the model grid as well as enter it.

The TRANS98 model is applicable only to non-cohesive sediments. Thus, the non-cohesive sediment pool in the model is represented by ten size classes with a mean of 88×10^{-6} m (3.5 ϕ). This study assumes that sand is entrained and transported independently of mud during the hurricane. This assumption is justified because mud remains in the water column much longer than coarser sediment. Consequently, in areas where sand and silt are significant, the simulated storm layer will consist of noncohesive sediment only.

2.2.1. The 1947 hurricane

The wind, wave, current and sedimentation simulations were completed for 18–19 September 1947 on a Cartesian grid of the Mississippi Bight area (Fig. 1A) with a horizontal resolution of approximately 800 m. The time step used for the SWAN wave model was 1 h. The resulting wave heights and periods outside of the estuary are reduced because of limited deepwater generation and propagation into Mississippi Bight. These weaker waves are considered reasonable for this study because of the focus on the shoreface and inside the barrier islands. The steady currents were calculated by the Princeton Ocean Model (POM) model (Oey and Chen, 1992). For this study, POM solves the vertically integrated equations for mass and momentum conservation using a time step of 6 s. The model does not include coastal flooding and drying. The sedimentation model was run on three sub-grids (Fig. 2) with the same resolution as the main grid.

2.2.2. Hurricane Camille

The wind, wave, current and sedimentation simulations were completed for 14–19 August 1969. The wind field for these simulations was calculated on a 5-km grid of the entire Gulf of Mexico. The wave model grid used by SWAN is the same as the wind grid. The resulting low resolution within Mississippi Bight is considered reasonable for this study because highly detailed wave fields are not necessary and cannot be validated. The steady currents were calculated by the ADCIRC-2DDI hydrodynamic model, the depth-integrated option of a set of two- and three-dimensional fully nonlinear codes named ADCIRC (Leuttich et al., 1992). ADCIRC-2DDI solves the vertically integrated equations for mass and momentum conservation on a grid with linear, triangular finite elements. The model as used in this study does not incorporate coastal flooding and drying. The model domain includes the entire Gulf of Mexico and the western North Atlantic, with resolution varying from 98 km in the open ocean to 500 m near tidal inlets (Blain, 1997). The steady currents from the ADCIRC model were used for Hurricane Camille because they had been computed as part of a previous study (Bentley et al., 2002). The

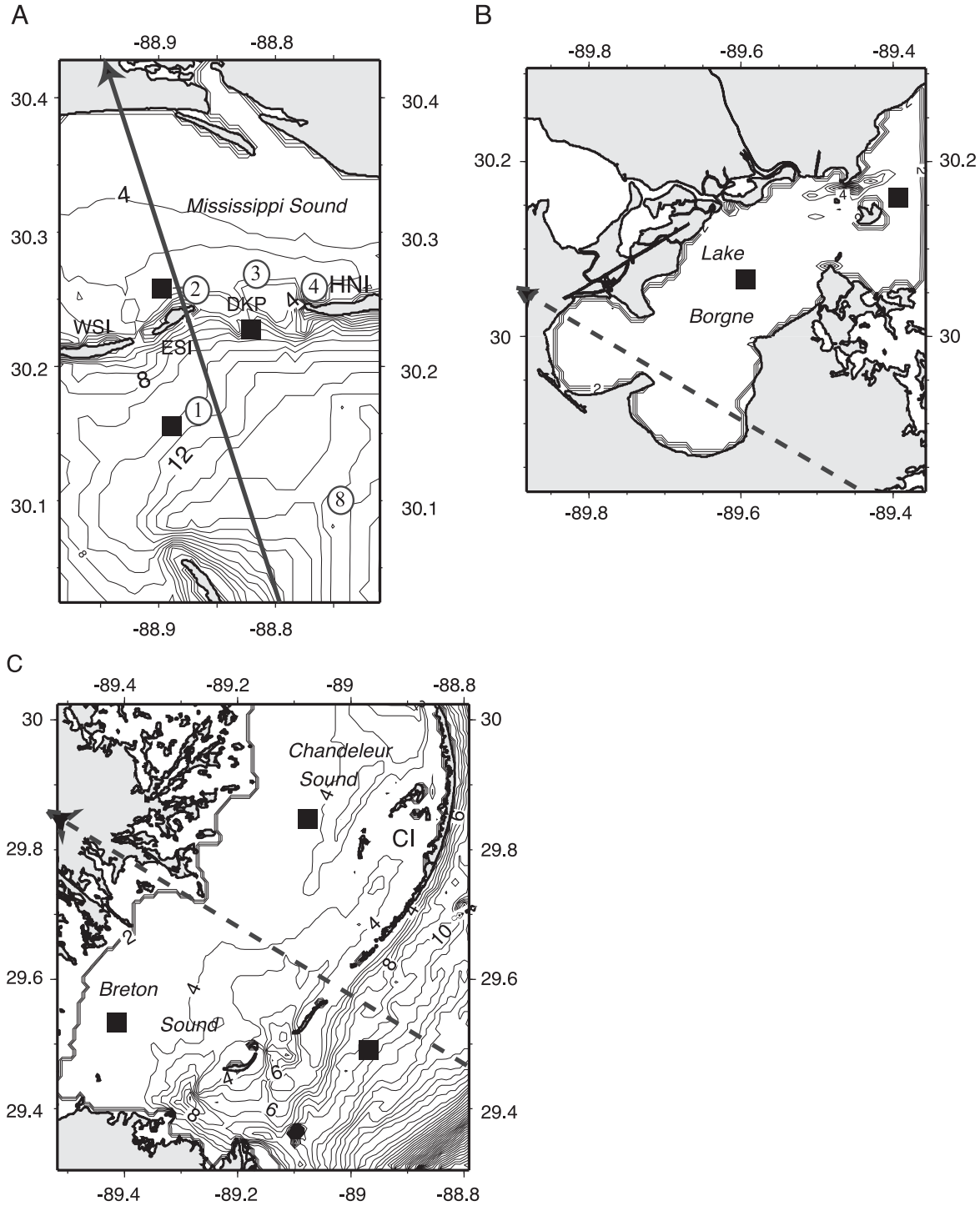

Fig. 2. Maps of sub-domains used for sedimentation model runs. (A) Central Mississippi Sound region. The path of Hurricane Camille is indicated by the solid line (WSI = West Ship Island; ESI = East Ship Island; DKP = Dog Keys Pass; HNI = Horn Island). (B) Western Mississippi Sound and Lake Borgne. The path of the 1947 hurricane eye is shown by the dashed line; and (C) The Breton Sound and Chandeleur Sound area (CI = Chandeleur Islands). The solid squares indicate the positions of simulated cores and time series discussed in text.

sedimentation model was run on the same grids (Fig. 2) as the 1947 hurricane.

2.3. Simulated stratigraphy

The changes in bed elevation calculated from Eq. (3) are used to define changes in the seafloor stratigraphy following Keen and Glenn (1998). When a net loss of mass occurs at a grid point because of advection, the resulting decrease in bed elevation is herein termed erosion. An increase in bed elevation associated with a net gain in mass is termed deposition. The resuspension depth is the equivalent thickness of sediment suspended in the water column when averaged over a wave period. The apparent bed thickness, which results from advection and resuspension, is the thickness of the sediment between the resuspension depth and the sea floor. This bed will be referred to as the sandy event layer hereafter. Note, however, that for a time interval less than the event duration, this bed represents both transported sediment within the bed and sediment in suspension above the bed. The simulated stratigraphy discussed in this paper will consist of this simulated sandy layer and mud layers estimated from field data.

The numerical sedimentation model was run independently for the two hurricanes. This approach assumes that the bottom sediment returns to a non-storm distribution between major storm events. This is reasonable since the storms are separated by 22 years. The stacking of the storm beds assumes that all of the mud will remain in suspension until the turbulence level has decreased to fair-weather conditions for some time. The consequence of this process is that a lag layer of sand is available to construct a storm bed independently of mud deposition. It follows that both the resuspension and erosion depths predicted by the model are independent of the noncohesive sediment content of the bed. This assumption is only valid if there are adequate quantities of sand and silt in the seabed, and if cohesive sediments at the water–sediment interface remain weak. Fine sand and silt are plentiful within the Mississippi Bight region, originating from Mobile Bay and other rivers within Mississippi Sound, and from the old St. Bernard delta underlying Chandeleur Sound.

The stratigraphic profile of each storm is comprised of three parts: (1) the sand layer, (2) the mud drape, and (3) mud deposited during fair weather after the storm. Bioturbation is overprinted on these three depositional units. The thickness of the sand layer is computed by TRANS98 using Eq. (3) as defined above. The mud drape is estimated as 0.04 m from core data as discussed below. A uniform fair-weather sedimentation rate of 1.5×10^{-3} m/year determined from ^{210}Pb profiles is used (Bentley et al., 2000, 2002), which is greater than the rate of 2.4×10^{-4} m/year suggested by Ludwick (1964) for the Holocene of Mississippi Sound. This rate is multiplied by the number of years between the two hurricanes, and from Hurricane Camille until the present. Bioturbation depths are highly variable and a single value of 0.06 m is used for the region. The reference level for the simulated cores is mean sea level (MSL). Depths are below MSL. The present discussion assumes no loss of sediment at any of the core locations. This is an oversimplification since muddy sediment would be transported by storm and fair-weather flows.

The simulated stratigraphic columns are produced in the following manner. The 1947 hurricane simulation is run to generate a sand layer. Then, the mud drape and fair-weather mud are deposited. The model predicts the depth of erosion and resuspension depths (see Keen and Glenn, 1998) to get the maximum depth of reworking, which represents the bottom of the storm sand layer. The Camille simulation is run independently and the model predictions are superimposed on the 1947 hurricane results. Thus, the bottom of the Camille sand layer may be below the bottom or top of the previous storm sand layer or anywhere within the overlying mud. The resulting simulated cores may consist of two discrete sand layers with intervening mud, two sand layers with no intervening mud, or one amalgamated sand bed. Undisturbed mud is deposited on top of the Camille bed. Bed preservation with respect to bioturbation is evaluated using a first-order finite difference model that describes the transformation from primary physical sedimentary fabric to biogenic sedimentary fabric as a function of burial rate and bioturbation rate (Bentley, 1998; Bentley and Nittrouer, 1999; Bentley and Sheremet, 2003). Conceptually, sediment deposited on the seabed initially possesses sedimentary fabric that is 100% physical in origin. Once an organism has ‘‘interacted’’ with physical fabric, whether by ingesting sediment or creating a

burrow, the modified fabric becomes irreversibly biogenic unless eroded. Thus, this model tracks the transformation of sedimentary fabric from physical to biogenic, rather than tracking sediment particles or a geochemical tracer. Bioturbation is portrayed as a first-order reaction, constant in time, having an exponential decrease of intensity with depth. The relevant equations are:

$$\frac{\Delta C_{z,t}}{\Delta t} = -\left[\frac{\omega_t \Delta C_{z,t}}{\Delta z}\right] - (\eta_z C_{z,t}) \quad (4)$$

Boundary conditions are applied, given by:

$$z = 0, J_{\text{sed}} = \omega C \quad (5)$$

$$z = L_{\text{b}}, \frac{\Delta C}{\Delta z} = 0 \quad (6)$$

where z = depth in sediment, ω = burial rate per year (annual deposition − annual erosion, cm year^{-1}), L_{b} = maximum depth of bioturbation, C = fraction of sediment volume at depth z and time t that is characterized by primary physical sedimentary fabric, J_{sed} is the flux of fresh sediment to the seafloor, and the depth-dependent volumetric bioturbation rate η (year^{-1}, or cm^3 cm^{-3} year^{-1}) is described by:

$$\eta(z) = \eta_0 \exp(-\alpha z), \quad (7)$$

where α is a depth-attenuation coefficient. The value for η can be interpreted as a decay constant, implying that half of the volume of sediment at depth z is mixed by an organism every $0.693/\eta_z$ years. Thus, the half-life of a sedimentary structure exposed to bioturbation at the rate of $\eta = 1$ is approximately 0.7 years. Bioturbation rates and depths were adapted from published bioturbation data from Western Mississippi Sound (Bentley et al., 2000); burial rate estimates were derived from $^{210}Pb_{xs}$ geochronology and event-layer development simulated by the models described above.

3. Results

3.1. Core analysis

3.1.1. Radioisotope geochronology

Core profiles of $^{210}Pb_{xs}$ (Fig. 3) show significant variability between stations. Individual profiles are generally irregular, lacking the gradual exponential decay with increasing depth that is associated with steady-state processes of sediment bioturbation and accumulation (Nittrouer and Sternberg, 1981; Bentley and Nittrouer, 1999). Gradients in the uppermost 0.05–0.10 m of all profiles vary widely. Physical and biological mixing processes tend to homogenize particle-bound radioisotopes and produce a reduced gradient of radioisotope activity with depth (Benninger et al., 1979; Dellapenna et al., 2000). Physical mixing and/or deposition are indicated by the faint bedding in the upper 0.05 m at station 5 (Fig. 4B) and at 0.07 m below sea floor (bsf) at station 1 (Fig. 4D). Numerous macrobenthos that were observed during core subsampling are also indicative of bioturbation. Other recent seabed studies of Mississippi Sound (Bentley et al., 2000) concluded that rapid bioturbation is limited to the upper 0.05–0.07 m, consistent with the $^{210}Pb_{xs}$ profiles. All of the $^{210}Pb_{xs}$ profiles in Fig. 3 contain a zone of nearly constant, or low but variable, activity at approximately 0.12 to 0.22 m bsf. The upper boundary of this zone varies from a sharp discontinuity at station 2 (Fig. 3B) to a change in gradient with no sharp discontinuity at station 4 (Fig. 3C). Higher surface activities at station 1 (Fig. 3D) are presumably associated with increasing $^{210}Pb_{xs}$ water-column inventories in high salinity waters offshore (Cochran, 1982).

Apparent sediment-accumulation rates were calculated for $^{210}Pb_{xs}$ profiles below the estimated depth of bioturbation after Nittrouer and Sternberg (1981). This approach assumes steady-state sediment accumulation, constant $^{210}Pb_{xs}$ activity at the seabed, and no bioturbation effects on the portion of the $^{210}Pb_{xs}$ profile for which the least-squares fit is conducted. Although it is unlikely that these conditions are met in Mississippi Sound, this approach provides a straightforward means for comparing profile shapes. The resulting estimate of the maximum rate of sediment accumulation averaged over the past 40 years ranges between 2.9×10^{-3} and 4.7×10^{-3} m year^{-1} for the profiles in Fig. 3. Maximum accumulation rates are 1.1×10^{-3} m year^{-1} for the middle shelf and 2.0×10^{-3} m year^{-1} for the outer shelf. No $^{210}Pb_{xs}$ was detected in cores from the Chandeleur Islands, probably due to the low affinity of ^{210}Pb for the coarse sediments in these cores.

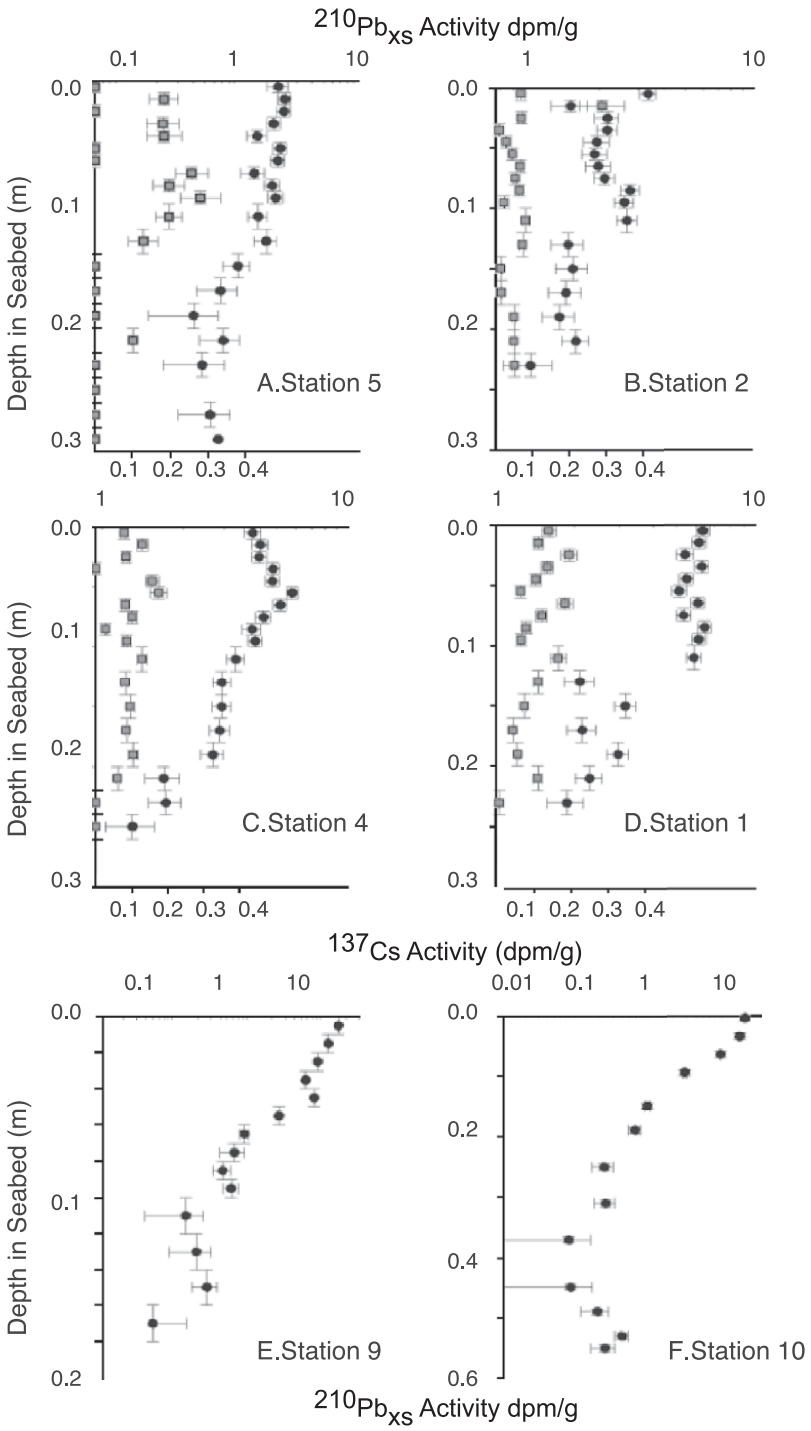

Fig. 3. Profiles of $^{210}Pb_{xs}$ (circles) and ^{137}Cs (squares) from box cores in the study area (see text for explanation).

Profiles of ^{137}Cs (squares in Fig. 3) show low and variable activities to depths of approximately 0.22 m at station 5, and 0.18–0.22 m bsf at station 2, below which ^{137}Cs is not detectable. ^{137}Cs is not detectable in cores from the Chandeleur Islands, and it is restricted to the upper 0.1 m of middle and outer shelf

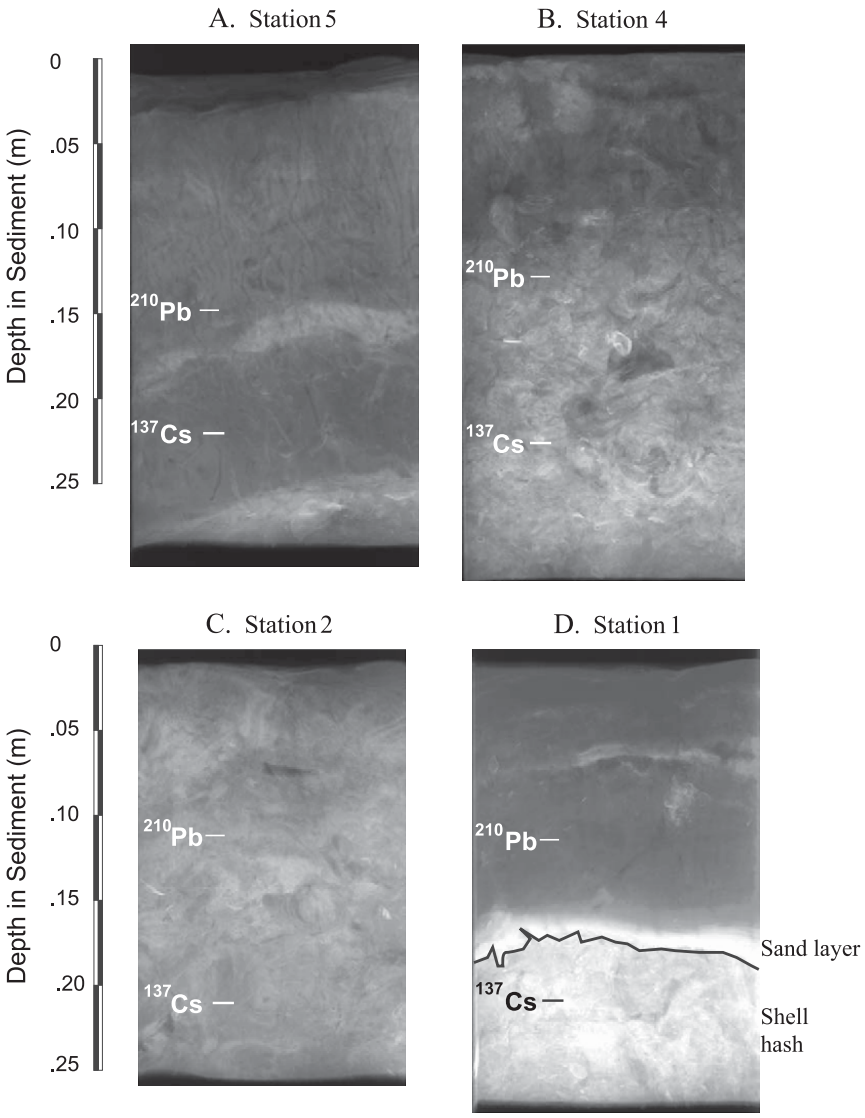

Fig. 4. X-radiograph negatives of box cores from the Mississippi Sound area. Bright zones correspond to zones with high bulk density (sand) and dark zones correspond to low bulk density (mud). For comparison with radionuclide profiles, the depth to disturbed areas of $^{210}Pb_{xs}$ profiles and maximum penetration depth of ^{137}Cs is indicated. The bottom of the sandy layer in panel D is indicated by a black line for clarity.

cores (not shown). The maximum penetration depth of ^{137}Cs cannot be used to calculate sediment accumulation rates in Mississippi Sound because of bioturbation and physical reworking during storms (Nittrouer et al., 1984; Bentley and Nittrouer, 1999; Bentley et al., 2002). In cores from Mississippi Sound and the adjacent inner shelf (station 1), the presence of ^{137}Cs at 0.18–0.22 m bsf demonstrates that some portion of the sediment at that depth has been deposited since the 1954–1963 time frame, even if ^{137}Cs-labeled particles have been mixed downward by physical and biological processes.

3.1.2. Physical properties

The sedimentary fabric in X-radiographs ranges from partially stratified at station 5 (Fig. 4A) and station 1 (Fig. 4D), to intensely bioturbated at station 2 (Fig. 4C). The X-radiographs reveal evidence of sandy layers at depths of 0.10–0.17 m bsf. The original sandy layers have been intermixed with muddier sed-

iment, however, to produce zones of higher bulk density, which show up as bright zones on the images. The sharpest contacts are preserved on the inner shelf, where a layer of laminated sand with a sharp basal contact at approximately 0.17 m bsf (indicated by a line in Fig. 4D) overlies coarser sediments with shell fragments. Biogenic fabric dominates at station 4 (Fig. 4B) and station 2. Mottling is produced by the density contrast between swirls of alternating sandy and muddy sediment.

The maximum penetration depth of ^{137}Cs and the depth of a sharp break in the $^{210}Pb_{xs}$ profiles are indicated on the X-radiographs in Fig. 4. In general, the depth interval bounded by the radionuclide profiles as discussed above coincides with sandy and sometimes physically stratified sediment in an otherwise muddy matrix in the X-radiographs.

The sand concentration was not determined for the cores shown in Fig. 4; however, the percent sand was measured in several cores collected near the cores discussed above (see Fig. 1 for locations). The sand concentration at station 6 (Fig. 5A) ranges from 20% to 50%, with maximum values at 0.04 m and 0.12–0.2 m bsf. The sand concentration at station 3 (Fig. 5B) is between 50% and 70%. The highest concentration occurs at the surface but sandy zones are also located at approximately 0.07 m and 0.17 m bsf (core depth is approximately 0.22 m). The sediment at station 4 (Fig. 5C) contains more mud, and the sand content ranges from 10% to 35%. Sandy zones are located at about 0.07 m bsf and between 0.1 and 0.25 m bsf (core depth is about 0.3 m). Although the cores shown in Fig. 5 were not collocated with the cores in Fig. 4, the depths to the maximum sand content are comparable to the bright zones seen in the X-radiographs.

Gamma density is a function of grain mineralogy, particle size, and water content and thus correlates with sand content in these cores. Maximum values for gamma density (Fig. 6) occur in each core between 0.15 and 0.25 m bsf. At stations 5 and 6 (Fig. 6A and B), two distinct maxima are evident. The gamma density data at station 1 (Fig. 6E) indicate sandy layers at 0.08–0.13 m and 0.17–0.29 m bsf separated by a muddy layer. More subtle subsurface gamma-density maxima are evident at station 2 (Fig. 6C) and station 4 (Fig. 6D). These maxima correspond in depth to sandy and/or bedded zones that are seen in X-radiographs and profiles of sand content (see Figs. 4 and 5). This indicates that maximum values of gamma density are associated with elevated sand content. The shaded areas in Fig. 6 display the overlap depth range of disturbed vertical $^{210}Pb_{xs}$ profiles (upper boundary of shaded area) and maximum penetration depths of ^{137}Cs (lower boundary of shaded area).

Gamma density profiles of cores collected near the Chandeleur Islands at stations 7 and 8 (Fig. 6F and G)

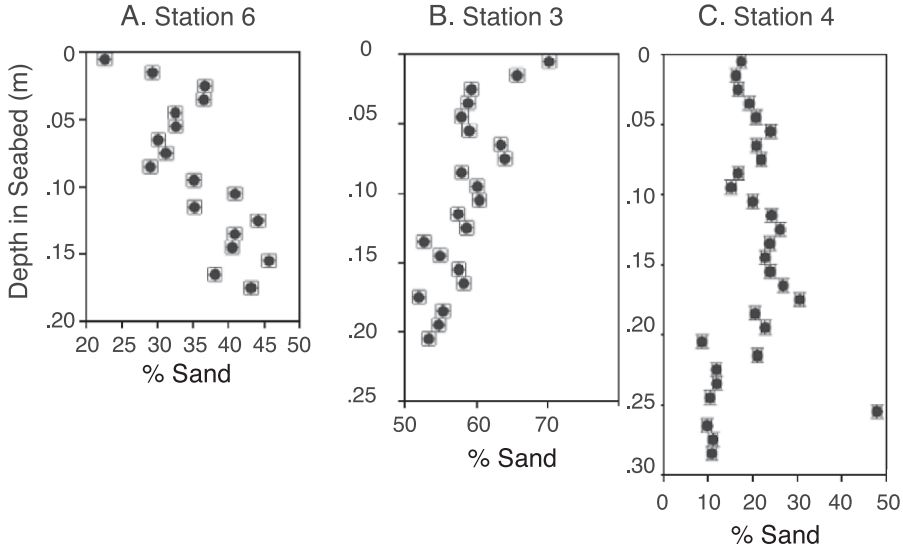

Fig. 5. Sand content of box cores from Mississippi Sound. The horizontal error bars indicate the standard deviation of three replicate measurements for one depth interval in each core.

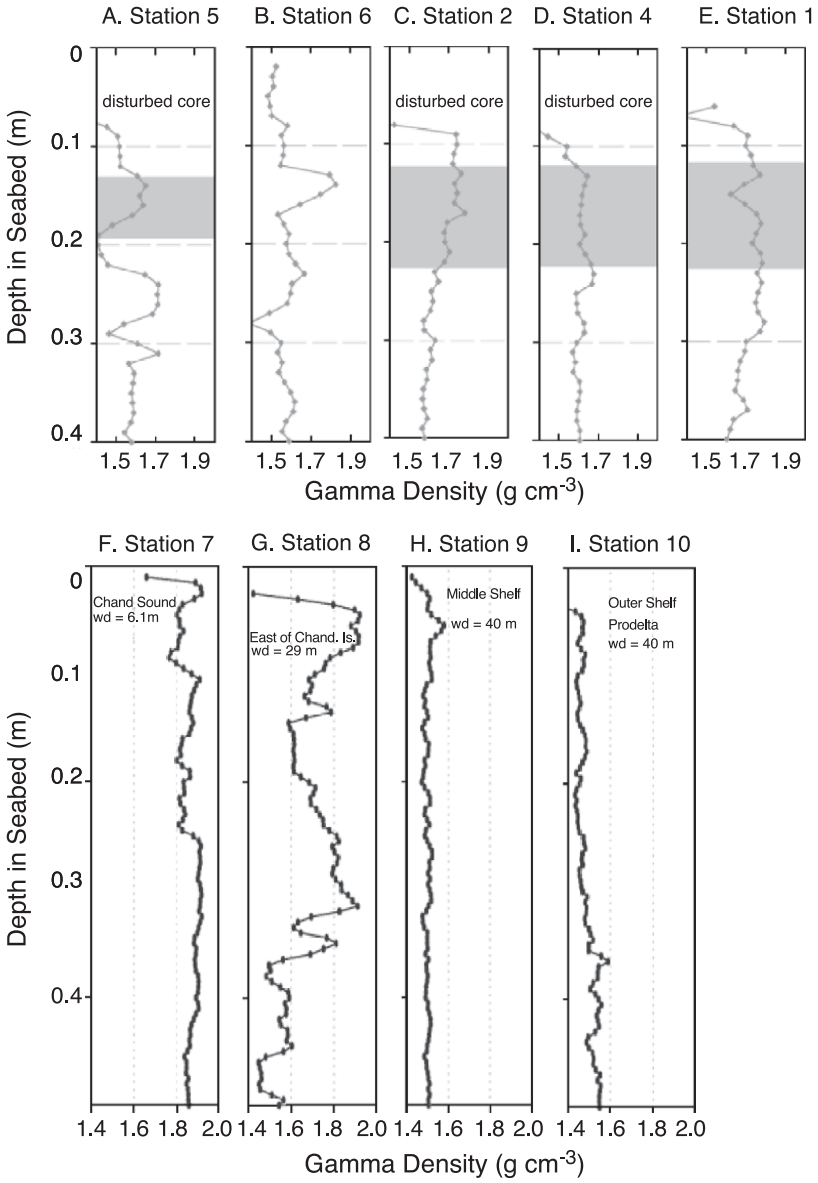

Fig. 6. Profiles of gamma density (g cm^{-3}) from gravity cores. The shaded area in panels A, C, D, and E indicates the disturbed $^{210}Pb_{xs}$ profile (upper boundary) and penetration depth of ^{137}Cs (lower boundary). See Fig. 1 for the locations of the stations.

have variable profiles with density maxima at approximately 0.05 and 0.15 m, and 0.25–0.35 m bsf. Unfortunately, a lack of $^{210}Pb_{xs}$ and ^{137}Cs chronology data prevents estimation of absolute ages for any of these beds. The gamma density profiles for the middle and outer shelf cores collected at stations 9 and 10 (Fig. 6H and I) have lower densities (approximately 1.5 g cm^{-3}), which vary significantly over vertical length scales of 0.05–0.1 m and are muddier than cores collected near the Chandeleur Islands. The low maximum accumulation rates for these cores imply that the upper 0.05–0.1 m of seabed has been reworked during the past 50 years.

3.1.3. Interpretation

Gamma density data from stations 5 and 6 indicate the presence of sandy layers at 0.12–0.18 and 0.23–0.29 m bsf in the western part of Mississippi

Sound. The uppermost layer must be younger than 1954 because it contains ^{137}Cs; it is thus likely from Hurricane Camille. Furthermore, the lower bed was probably deposited by the 1947 hurricane. Two sandy layers are also evident at station 1, which is south of Ship Island. The inferred Camille bed is at 0.08–0.13 m bsf, and the probable 1947 hurricane bed is located at 0.17–0.29 m bsf.

Radiochemical and fabric analyses show that the initial 1947 and Camille storm beds in western Mississippi Sound consisted of sandy basal layers approximately 0.05 m thick with overlying mud drapes 0.05–0.1 m thick (Bentley et al., 2000, 2002). Disruption by bioturbation destroyed primary bedding in the mud drape of both beds, however. The basal sandy layer is also truncated and only discontinuous sandy lenses with faint internal lamination in a bioturbated muddy matrix are preserved. The same observations hold for the cores collected near Horn Island (station 4), East Ship Island (station 2) and the adjacent inner shelf (station 1). Fabric evidence (Fig. 4) shows that post-depositional bioturbation has destroyed most primary stratification at stations 2 and 4 in the central part of Mississippi Sound. A zone of bioturbated sandy mud is sandwiched between zones of bioturbated muddy sand in these cores. Consequently, the best evidence for initial bed geometry for these cores comes from ^{210}Pb$_{xs}$ and ^{137}Cs data.

The Camille bed contains a preserved radiochemical signature that is characterized by an upper boundary marked by a discontinuity in the ^{210}Pb$_{xs}$ profile. The lower boundary is marked by the maximum depth of ^{137}Cs. ^{210}Pb$_{xs}$ activities are relatively constant within the bed. Using these criteria, the initial thickness of the bed was at least 0.1 m, including both the mud drape and basal sandy zone, and it was located at 0.12–0.22 m bsf (Figs. 3 and 4).

Cores from the Chandeleur Islands (stations 7 and 8), middle shelf (station 9), and outer shelf (station 10) are not suitable for such high-resolution geochronology because of low or undetectable activities of radiotracers. However, gamma density logs show significant stratigraphic variation within individual cores, indicating that the seabed at these locations was exposed to fluctuations in the intensity of reworking through time.

3.2. Numerical model results

The numerical sedimentation model TRANS98 is used in this study to predict the initial properties and distribution of the two hurricane event beds in Mississippi Bight. The model is run in three areas (Fig. 2): (1) the central part of Mississippi Sound and the adjacent shelf; (2) the western end of the sound and in Lake Borgne; and (3) Chandeleur and Breton Sounds to the southwest. These three areas were selected to examine event layer stratification in different environments rather than to reproduce the field stations discussed above. Therefore, the model output will not be referred to by station number because that would imply a direct correspondence to the core stations. The locations of model output discussed below are indicated by squares in Fig. 2.

3.2.1. Central Mississippi Sound

The 1947 hurricane made landfall in Breton Sound but the largest waves computed by SWAN (Fig. 7A) are predicted on the open shelf south of Ship Island (dotted line). Maximum significant wave heights are more than 1.4 m near Ship Island (solid line). The predicted wave period (Fig. 7B) in the sound is more than 7 s at the storm maximum. The simulated currents (Fig. 7C) inside Mississippi Sound reach 1.2 m s^{-1} during the storm buildup phase before decreasing as the eye made landfall. Currents increase to 1 m s^{-1} as the storm surge ebbs. The first pulse is associated with landward flow while the second is seaward. The predicted bed shear velocity $u^*_{cw}=(\tau/\rho)^{1/2}$, where τ is the wave–current shear stress and ρ is density of seawater, is moderate near Ship Island and much higher on the open shelf.

The simulated initial sand layer deposited by the 1947 hurricane (Fig. 8A) is less than 0.1 m thick over most of the central Mississippi Sound area. Thick beds are deposited near the islands because of the landward boundary condition used in TRANS98, which supplies plentiful sand. The original storm layer is subsequently modified during the passage of Hurricane Camille in 1969, and the post-Camille thickness of the 1947 sand layer (Fig. 8B) is less than 0.05 m everywhere except on the shelf. It is about 0.02–0.03 m inside Mississippi Sound. It has a highly irregular appearance on both sound and seaward sides of Dog Keys Pass. A 0.2-m-thick bed

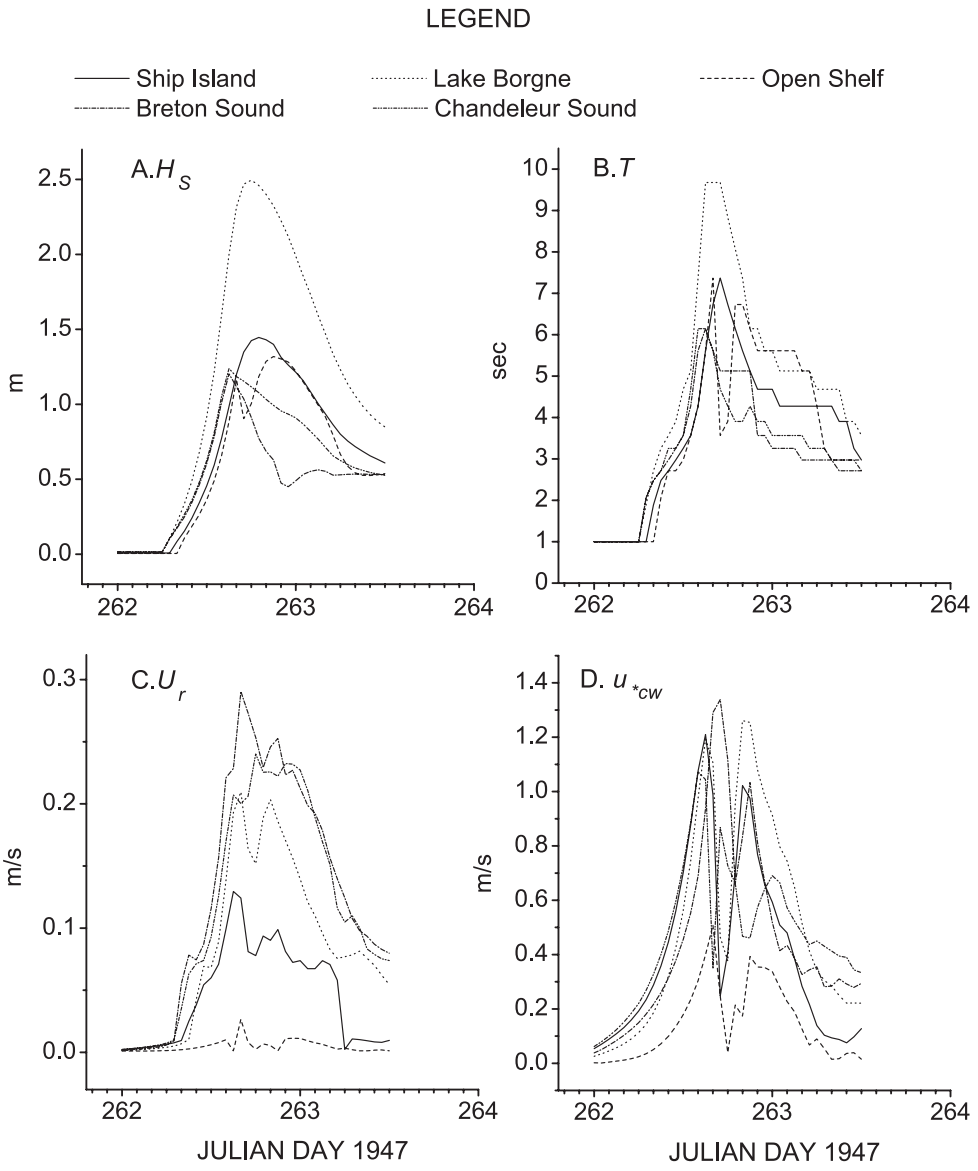

Fig. 7. Time series of simulated significant wave height (m) (A), peak wave period (s) (B), current speed (m s^{-1}) (C), and shear velocity (m s^{-1}) (D) at different locations within the Mississippi bight during the 1947 hurricane. See Fig. 2 for locations.

is preserved at Dog Keys Pass and at the northern tip of the Chandeleur Islands.

Hurricane Camille passed directly over Ship Island and the simulated storm waves (Fig. 9A) reach 3.8 m on the inner shelf south of Ship Island (dotted line). The waves within Mississippi Sound (solid line) are much lower. The predicted wave period (Fig. 9B) in the open gulf (not shown) is constant throughout the hurricane at more than 18 s, whereas the wave period is 6 s near Ship Island. Steady currents (Fig. 9C) on the inner shelf exceed 1.3 m s^{-1} during the storm. Two peaks are predicted inside the sound, with the larger flow occurring during the ebbing tide. Because of the large waves on the shelf, the shear velocity (Fig. 9D) predicted by TRANS98 is more than 0.4 m s^{-1}. Smaller shear stresses are predicted inside the sound.

The post-storm thickness of the simulated Camille sand layer in central Mississippi Sound (Fig. 8C) is much greater than the 1947 hurricane because of the

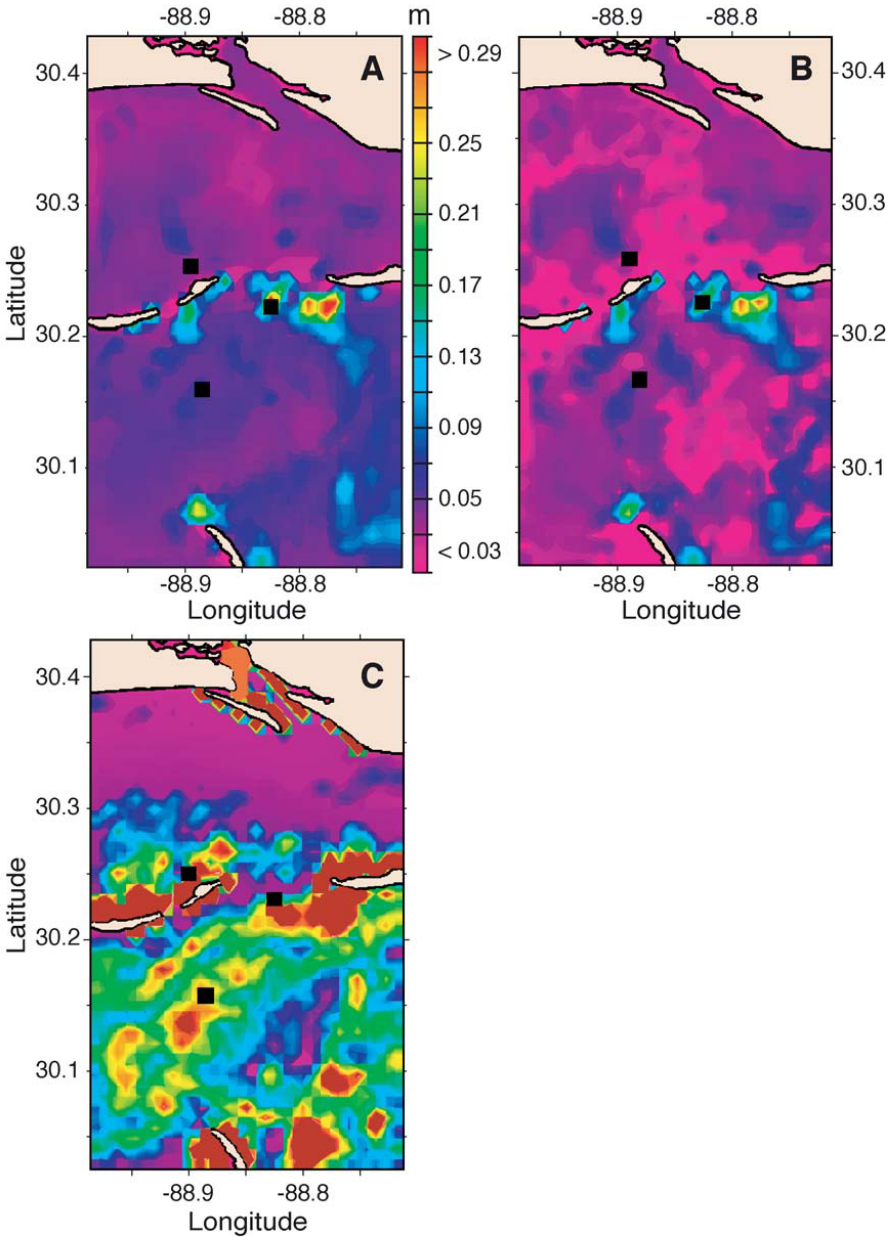

Fig. 8. Contour plots of simulated hurricane sand layers from the central Mississippi Sound model grid. (A) Thickness (m) of the sand layer immediately after the 1947 hurricane. (B) Thickness (m) of the 1947 hurricane sand layer after resuspension and erosion by Hurricane Carla. (C) Thickness of the Hurricane Camille sand layer. The solid squares indicate the positions of simulated cores and time series discussed in text.

proximity of landfall. The sand layer inside the sound is less than 0.05 m along the landward coast, thickening to more than 1 m on the landward sides of the barrier islands. The bed thins to less than 0.1 m between Ship and Horn Islands because of seaward transport by the ebbing storm surge. The sand layer on the shelf is 0.2–0.3 m in thickness.

Simulated cores are constructed as described in the Methods section. The core from inside the sound near the eastern end of Ship Island (Fig. 10A) reveals no preserved bed from the 1947 hurricane or fair-weather mud deposition. The Camille sand bed is almost 0.3 m thick, with a mud drape of 0.04 m and an equal amount of post-1969 deposition.

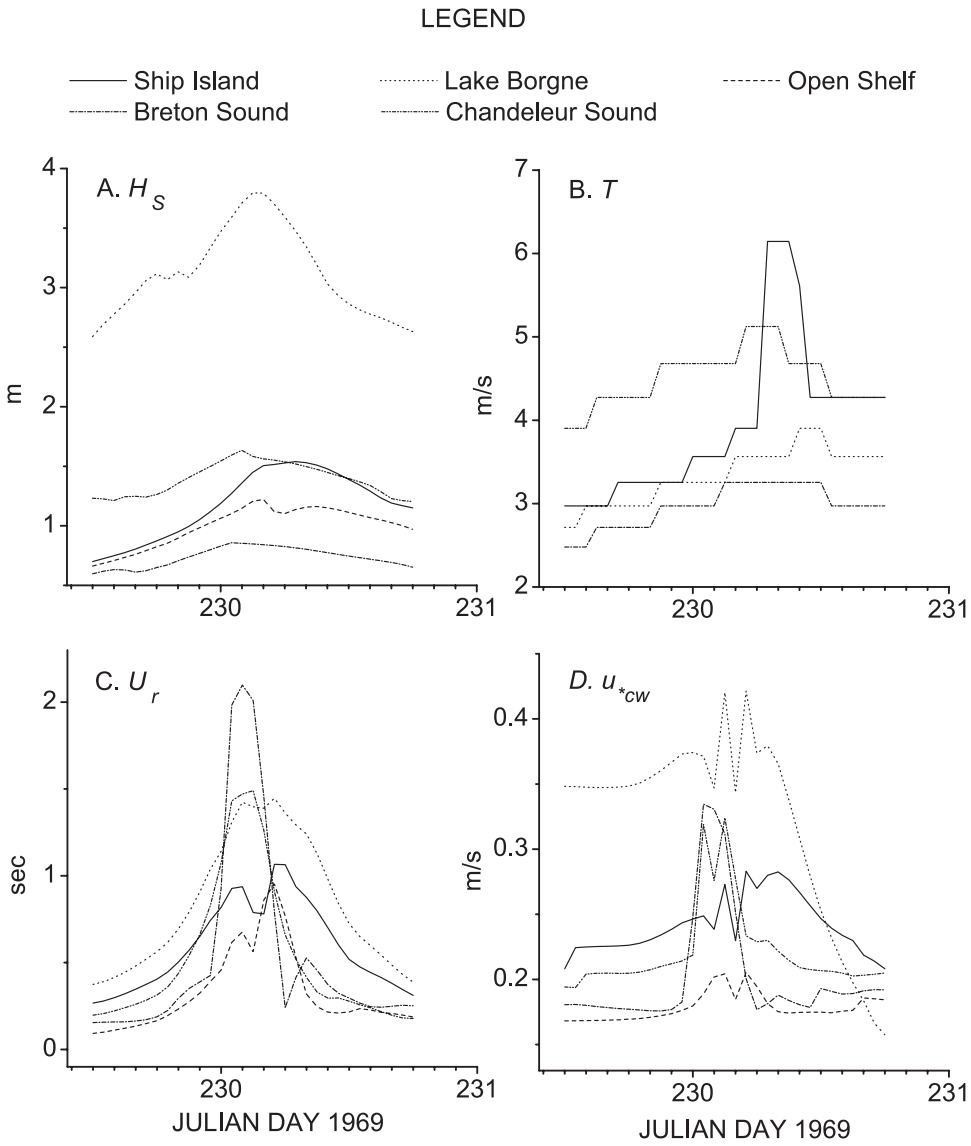

Fig. 9. Time series of simulated significant wave height (m) (A), peak wave period (s) (B), current speed (m s^{-1}) (C), and shear velocity (m s^{-1}) (D) at different locations within the Mississippi bight during Hurricane Camille. See Fig. 2 for locations.

The simulated stratigraphy on the shelf (Fig. 10B) reveals two sand layers. The lower bed is the 1947 hurricane layer, which is less than 0.04 m in thickness, whereas the upper (Camille) layer is 0.15 m thick. Both the mud drape and part of the post-1947 sediment are preserved. A core from within Dog Keys Pass (Fig. 10B) shows the stacking of 0.2-m-thick sand layers from the two storms with no intervening mud.

3.2.2. Western Mississippi Sound and Lake Borgne

Coastal water setup during the 1947 hurricane is greatest in western Mississippi Sound and Lake Borgne, with a maximum of 4 m predicted by POM. The relatively large waves in Lake Borgne (dashed line in Fig. 7) are possible because of the storm surge, which doubles the depth of the lake. The predicted storm waves also have a peak period of more than 7 s. The maximum shear velocity is greater than 0.02 m

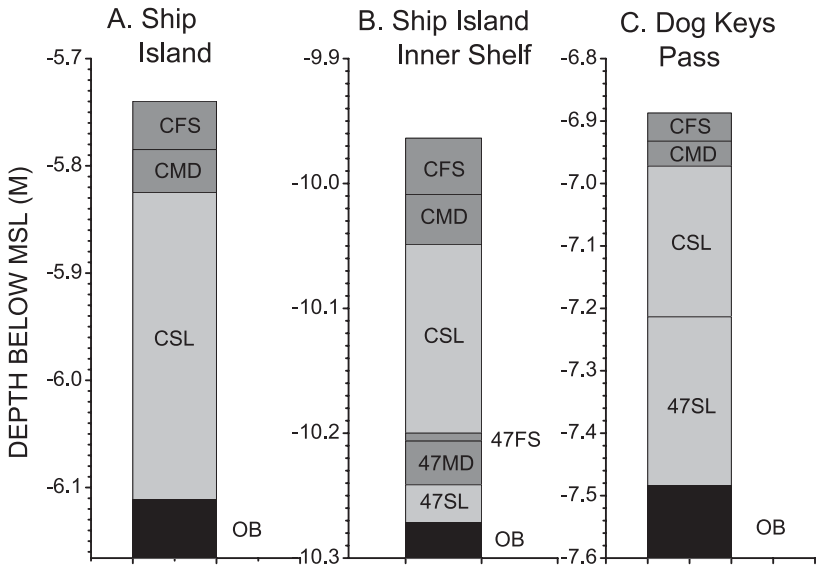

Fig. 10. Simulated cores from central Mississippi Sound: (A) Ship Island; (B) the inner shelf; (C) Dog Keys Pass. See Fig. 2 for locations. Key to abbreviations: OB = original bed; 47SL = 1947 hurricane sand layer; 47MD = 1947 hurricane mud drape; 47FS = fair-weather sediment between 1947 and 1969; CSL = Camille sand layer; CMD = Camille mud drape; CFS = post-1969 fair-weather sediment.

s^{-1} for only a short time, however, because the model currents never exceed 0.5 m s^{-1}. The 1947 sand-layer is not excavated by Hurricane Camille in the center of Lake Borgne, however, and the preserved sand layer is identical to the original except at the margins. This bed (Fig. 11A) thins near the margins of Lake Borgne. It exceeds 0.025 m in the narrow pass between the lake and western Mississippi Sound.

The predicted Hurricane Camille storm waves within Lake Borgne (dashed line in Fig. 9A) are less than 1.4 m and the peak period never exceeds 4 s, because of the small storm surge in this area. Steady currents are greater than 0.9 m s^{-1}, which is larger than for the 1947 hurricane. Consequently, the maximum shear velocity is greater than 0.2 m s^{-1}. The landward boundary condition used in TRANS98

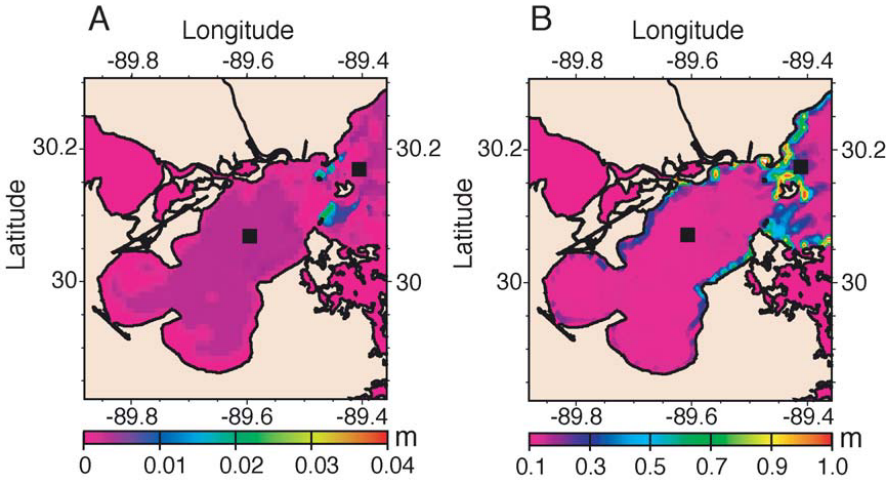

Fig. 11. Contour plots of simulated hurricane sand layers from the western Mississippi Sound model grid. (A) Thickness (m) of the 1947 hurricane sand layer after resuspension and erosion by Hurricane Carla. (B) Thickness (m) of the Hurricane Camille sand layer. The solid squares indicate the positions of simulated cores and time series discussed in text.

assures that predicted shoreface deposition will be significant during the storm; consequently, the sand layer exceeds 0.3 m at the northern and southern coasts and reaches almost 1 m at the eastern entrance to the lake (Fig. 11B).

A simulated core from the western end of Mississippi Sound (Fig. 12A) indicates the importance of Hurricane Camille within the sound. The 1947 hurricane sand layer is less than 0.01 m thick, but the mud drape and part of the 1947–1969 sediments are preserved. More than 0.13 m of sand is deposited during the Camille simulation, despite the lack of significant disturbance of the older storm bed. Lake Borgne is protected from the brunt of the storm waves during both hurricanes. Consequently, the sand layers (Fig. 12B) are much thinner and the simulated core is dominantly mud.

3.2.3. Chandeleur and Breton Sounds

The predicted largest storm waves during the 1947 hurricane are very similar (about 1.2 m) in Breton Sound (dot-dashed line in Fig. 7) and Chandeleur Sound (dot-dot-dashed line in Fig. 7) because of restricted wave fetch and shallow water depths. The wave period predicted by SWAN is just over 6 s. The

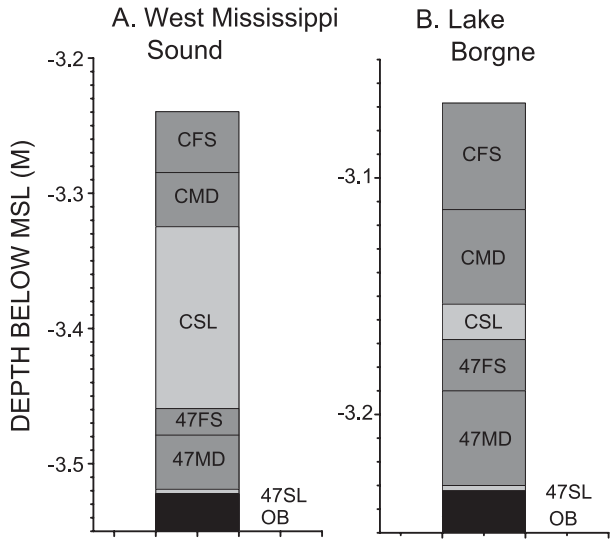

Fig. 12. Simulated cores from western Mississippi Sound: (A) the western end of the sound; (B) Lake Borgne. See Fig. 2 for locations. Key to abbreviations: OB = original bed; 47SL = 1947 hurricane sand layer; 47MD = 1947 hurricane mud drape; 47FS = fair-weather sediment between 1947 and 1969; CSL = Camille sand layer; CMD = Camille mud drape; CFS = post-1969 fair-weather sediment.

storm flow in Breton Sound exceeds 1.3 m s^{-1}, which is the largest within the region, but currents in Chandeleur Sound are also more than 1 m s^{-1}. The storm surge is low but the resulting smaller storm waves nevertheless have a significant impact on the model bed, especially in conjunction with the large currents. Consequently, the calculated shear velocity exceeds 0.29 m s^{-1} in Breton Sound and 0.24 m s^{-1} in Chandeleur Sound.

The 1947 hurricane passed directly over Breton Sound, and shoreface deposition predicted by TRANS98 is extensive because of the landward boundary condition for sediment transport. However, the simulated initial sand layer (Fig. 13A) is less than 0.04 m within this area because much of the sediment eroded from within the sound is transported to the inner shelf, where sand deposition exceeds 0.6 m. Deposition within Chandeleur Sound takes the form of large linear sand waves oriented perpendicular to the dominant flow direction. The sand layer in the troughs is less than 0.02 m thick. The crests contain as much as 0.4 m of sand. The simulated 1947 storm bed is modified by Hurricane Camille and the preserved bed (Fig. 13B) is much thinner near the pass at the southern end of the Chandeleur Islands.

The modeled storm waves during Hurricane Camille are less than 1 m in height within Breton Sound (dot-dashed line in Fig. 9) and the peak period is less than 3.5 s. The waves within Chandeleur Sound (dot-dot-dashed line) are much larger. The ADCIRC-predicted steady currents in Breton Sound exceed 2 m s^{-1}, however, and the maximum shear velocities computed by TRANS98 are greater than those in Chandeleur Sound. The shear stresses within this region are large enough to entrain most sediment throughout the storm. Consequently, the preserved Camille sand bed (Fig. 13C) is more than 0.03 m thick throughout this area. Local beds exceed 1 m near the islands and on the north side of the Balize delta.

A simulated core from Breton Sound (Fig. 14A) contains two thin sand beds. The lower bed is 0.025 m thick and the upper bed is approximately 0.03 m thick. The sequence is capped by mud. Sand is plentiful from the Chandeleur Islands and, consequently, the simulated core from Chandeleur Sound (Fig. 14B) contains a 0.185-m amalgamated sand bed overlying the remnant of the 1947 sand layer. Much of this sand

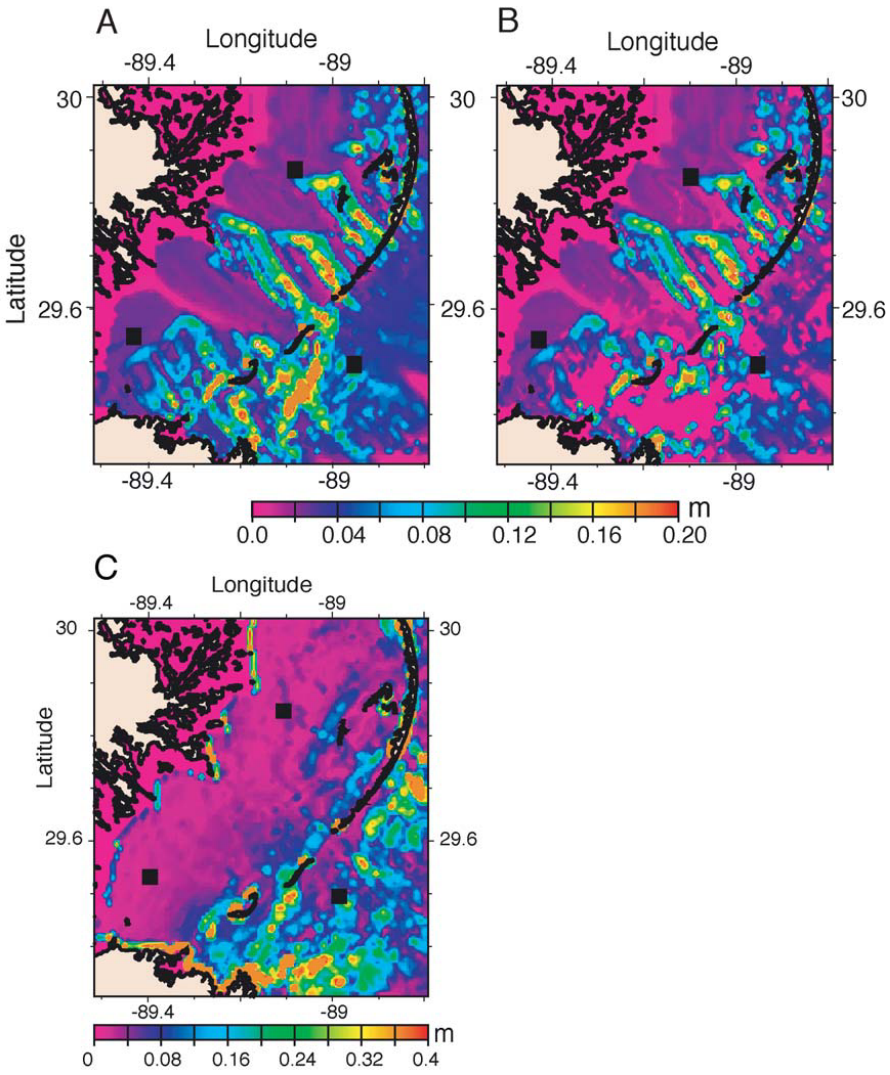

Fig. 13. Contour plots of simulated hurricane sand layers from the Chandeleur Sound model grid. (A) Thickness (m) of the sand layer immediately after the 1947 hurricane. (B) Thickness (m) of the 1947 hurricane sand layer after resuspension and erosion by Hurricane Carla. (C) Thickness (m) of the Hurricane Camille sand layer. The solid squares indicate the positions of simulated cores and time series discussed in text.

is removed from the barrier islands during both storms. The simulated core from the open shelf near the Chandeleur Islands (Fig. 14C) resembles that from the inner shelf near Ship Island (Fig. 10C) but the sand layers are slightly thinner.

3.2.4. Comparison of simulated and measured cores

The numerical models are used in this study to examine the relationships between the environmental forcing and the deposition of a sandy bed during the hurricanes. They can be used to constrain the distribution of such a bed throughout the region because of their use of physics rather than gross parameterizations. However, there are many simplifications and assumptions inherent in such an approach, which make it difficult to attempt a direct comparison between the simulated event layer and that observed in cores. For example, the bottom shear stress is sensitive to small variations in the current and wave field. The large cell size (650 m) used by TRANS98 cannot resolve the actual bottom stress field and resulting sedimentation during the storms. The treatment of the landward

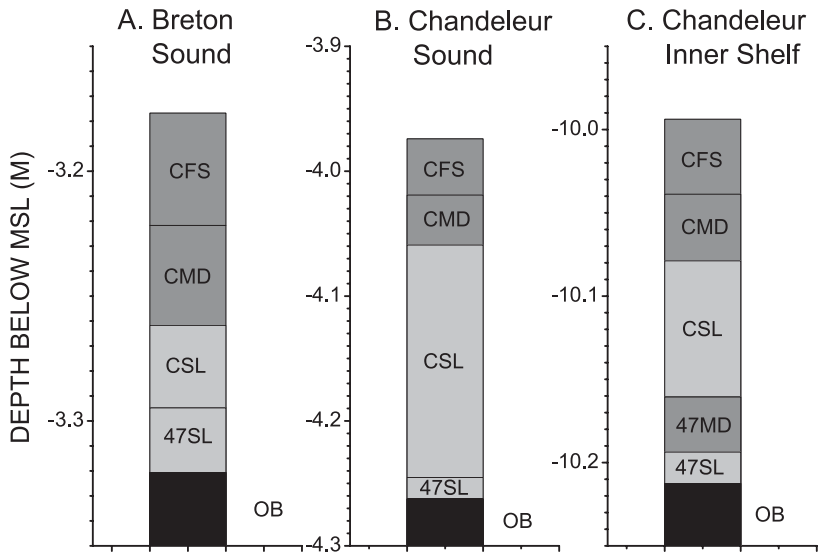

Fig. 14. Simulated cores from Chandeleur Sound: (A) Breton Sound; (B) Chandeleur Sound; (C) the adjacent inner shelf. See Fig. 2 for locations. Key to abbreviations: OB = original bed; 47SL = 1947 hurricane sand layer; 47MD = 1947 hurricane mud drape; 47FS = fair-weather sediment between 1947 and 1969; CSL = Camille sand layer; CMD = Camille mud drape; CFS = post-1969 fair-weather sediment.

boundary condition is also quite different from the reality of the storm surge overtopping the barrier islands and allowing storm waves to erode otherwise subaerial sediments. Nevertheless, if these warnings are kept in mind, it is reasonable to make limited quantitative and qualitative comparisons between the observed and simulated cores. This exercise serves to verify if the model is a reasonable approximation to the storm sedimentation system and indicate possible improvements to the model.

The simulated cores from Ship Island and Dog Keys Pass (Fig. 10A and C) indicate a predominance of amalgamated, sandy beds ranging from 0.37 to 0.51 m in thickness. These simulated cores can be compared to the cores collected at stations 2 and 3, respectively. Station 4, which is near Horn Island, is also close to the model output location at Dog Keys Pass. The measured cores from stations 2 and 4 (Fig. 4B and C) are bioturbated but show an increase in sand content with depth. This pattern is similar to the simulated cores, which contain a mud cap above the Camille bed. The total Camille bed at these stations, which is bounded by the ^{210}Pb and ^{137}Cs limits in Fig. 4, is 0.1 m. The simulated stratigraphy is condensed at Dog Keys Pass but the total Camille bed is 0.24 m, whereas the amalgamated Camille bed at Ship Island is 0.33 m. The thicknesses of the storm beds predicted by the model at these locations are thus too large by a factor of 2 to 3, probably because of their proximity to the barrier islands and the resulting effect of the landward boundary condition.

The simulated core from western Mississippi Sound (Fig. 12A) can be compared to the cores from stations 5 and 6, which are located approximately 10 km to the northeast. The simulated core contains two storm layers; the 1947 storm bed is 0.04 m thick and the Camille bed is 0.18 m thick. The X-radiograph of the core collected at station 5 (Fig. 4A) reveals two distinct sandy layers, which are verified by the gamma density data at both this station and station 6 (Fig. 6A and B). These storm beds have total thicknesses of 0.1 to 0.15 m for the 1947 hurricane and Camille, respectively. This comparison is relatively robust because of the preservation of the sandy layers in the cores.

The sedimentation model produced simulated cores at two locations on the inner shelf, one south of Ship Island and one southeast of the southern Chandeleur Islands (see Fig. 2 for locations). The inner shelf simulated core from near Ship Island is located near station 1. This simulated core contains a 1947 storm bed that is 0.07 m thick and a Camille bed that is 0.15 m thick. The X-radiograph of the core from station 1 (Fig. 4D) reveals a sandy layer, which would presumably be the Camille sand bed, overlying a shell deposit. The

thickness of the 1947 and Camille storm beds can be estimated from the gamma density profile in Fig. 6E; the 1947 bed is 0.12 m thick and the Camille bed is estimated as 0.05 m in thickness. The similarity of the simulated and measured cores is evidence that the model has captured the critical environmental forcing and sedimentary response. It is noteworthy that both the model and the measurements indicate preservation of the older storm deposit at this location. The more southerly simulated core is from a water depth of approximately 10 m, but it can be compared qualitatively to station 10, which is located 30 km to the east in a water depth of 59 m. The measured gamma density at station 10 (Fig. 6I) indicates faint stratification in the upper ~ 0.15 m of the core, which has been deposited and/or reworked during the last 50 years, based on ^{210}Pb geochronology. The simulated core from the inner shelf (Fig. 14B) contains a total of 0.19 m of reworked sediment from both hurricanes.

3.3. Biogenic destruction of primary fabric

Bioturbation is an important process in the post-depositional modification of sedimentary fabric; however, very few bioturbation measurements that can be used to model bed destruction have been made. Available observations from the northern Gulf of Mexico (Bentley et al., 2000) indicate that the upper 0.06–0.1 m of the seabed is subject to the most rapid bioturbation and that the upper 0.01–0.05 m can be mixed completely over timescales of 2 to 12 months. Accordingly, we have assigned relatively shallow bioturbation depths ($L_b = 0.06$ m, Eq. (3)) for regions with lower salinity and more restricted circulation (western Mississippi Sound and Lake Borgne), and deeper bioturbation depths for more oceanic or less restricted regions ($L_b = 0.1$ m for Dog Keys Pass, Ship Island, and the inner shelf). Following the same reasoning, a relatively low bioturbation rate ($\eta_0 = 1$ year^{-1}, Eq. (4)) has been assigned to the most restricted setting, Lake Borgne, and a higher bioturbation rate ($\eta_0 = 2$ year^{-1}) has been assigned to the other stations.

Because of the limited data available for estimating sediment flux and associated burial rates, the temporal resolution of the model is coarse, particularly in treating burial rates associated with the 1947 and Camille hurricanes. Nevertheless, the results (Fig.

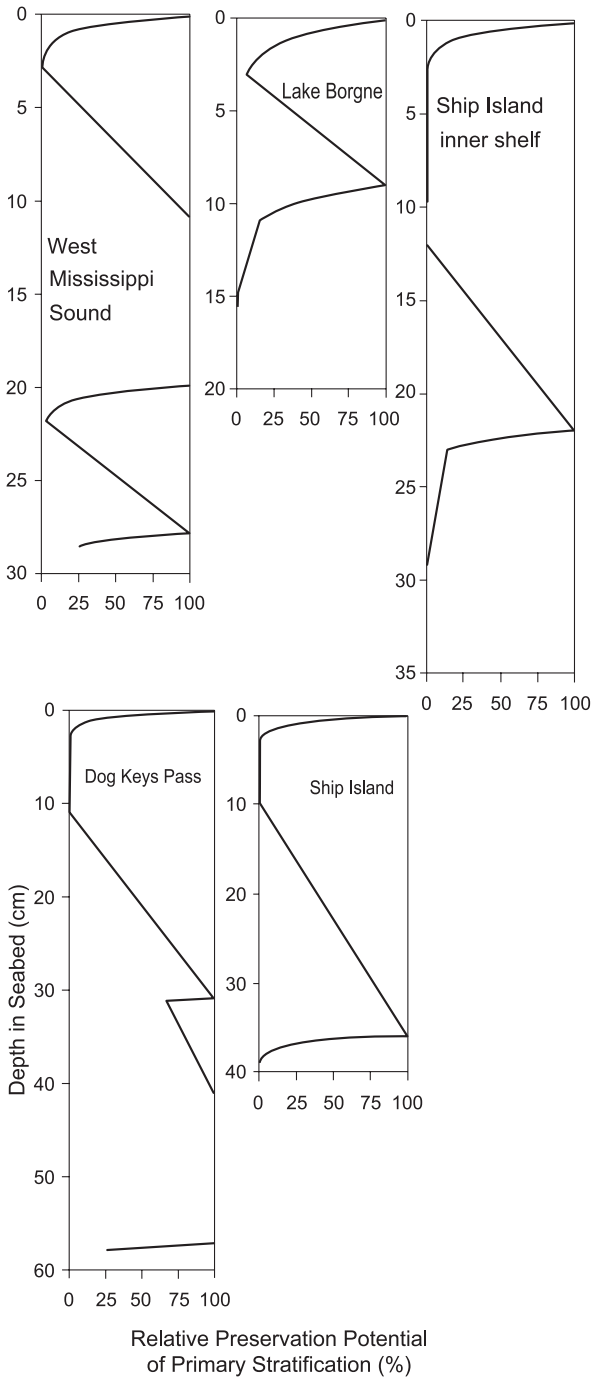

Fig. 15. Simulated core profiles of preservation potential for primary physical stratification, as a function of burial rate and bioturbation rate and depth (Eqs. (4)–(7)), for selected locations. Burial rate estimates are derived from ^{210}Pb and ^{137}Cs geochronology and bed thickness predicted by numerical modeling (Figs. 12–14). Bioturbation rate and depth are derived from regional experimental and observational studies explained in the text.

15) show significant lateral variability in the degree of preservation for both the 1947 storm bed and the Camille bed. Interpretation of the bioturbation results assumes that unbioturbated sediments would preserve sharply alternating beds of mud and sand, and that bioturbation mixes sand and mud across bed contacts. Given this assumption, the results generally conform to the distribution of bedding preserved in X-radiographs (Fig. 4) and implied by the gamma density logs (Fig. 6). Based on these simulations, it is only in western Mississippi Sound and Dog Keys Pass that we anticipate preservation of clearly identifiable beds for both the 1947 hurricane and Camille. In the case of Dog Keys Pass, the sandy character of both the 1947 and Camille beds would make it difficult to identify the intervening boundary. In both cases, preservation of the primary depositional fabric is permitted because the event beds are thicker than the depth of biogenic mixing, thus allowing basal portions of the beds to escape bioturbation. Where initial bed thickness is comparable to or less than the bioturbation depth, the preservation potential for primary fabric is poor, as for the Lake Borgne and inner shelf bioturbation simulations. In these locations, the bed produced by the 1947 storm (0.11–0.15 and 0.23–0.29 m bsf, respectively) would have been almost totally disrupted by subsequent bioturbation. Finally, our simulations appear to overestimate the degree of preservation of the Camille bed in western Mississippi Sound and possibly other locations. This occurs in part because the simulated bed thickness is greater than that observed in the cores, but it may also arise if bioturbation extends deeper than the 0.06–0.1 m depth used for our model.

4. Discussion

4.1. Event bed deposition

Hurricane beds are generated in two stages (Aigner and Reineck, 1981; Snedden and Nummedal, 1990). First, a sandy basal layer is produced by resuspension, erosion, advection, and deposition of coarse sediment. Second, a mud drape is deposited during the waning stages of the storm and during the following days. This secondary sedimentation also includes both coarse and fine sediment from river runoff associated with storm rainfall. The numerical model is used to simulate the first stage whereas deposition of the mud drape has been estimated from observations within the region.

The generation of a sandy event bed is controlled by several factors, including storm waves and currents, water depth, the coastline, and the availability of sandy sediments. External forcing factors, as represented by the storm strength and path, are filtered by the local bathymetry and coastline. For example, Breton Sound is 50 km from the track of Hurricane Camille and directly along the 1947 hurricane path. Consequently, the maximum hindcast wave height is approximately 1.25 m for the 1947 hurricane (Fig. 7) but less than 1 m for Camille (Fig. 9). However, the peak hindcast current is more than 2 m s^{-1} during Camille, compared with less than 1.4 m s^{-1}. Chandeleur Sound lies directly between the two storm tracks. The maximum waves for each storm are approximately 1.3 m but the Camille currents are 1.5 m s^{-1}, compared to less than 1.1 m s^{-1} for the 1947 hurricane. Surprisingly, the maximum hindcast waves for both hurricanes at Ship Island are 1.5 m, although Camille passed directly over the island. The major difference between the simulated coastal oceanographic responses to the two storms is the 7-m storm surge produced by Camille, which was caused by its direct approach to Mississippi Sound. This greater storm surge generated stronger flow within the estuary and thus more sediment transport. Peak storm waves were similar for the two hurricanes and, therefore, the storm currents were the dominant factor differentiating the sandy event layers from these two storms.

The availability of sand is a major limiting factor in the deposition of a sandy event layer. The modeling approach used in this study assumes that mud goes into suspension and remains there until well after the hurricane. This implies that a sufficient quantity of sediment is entrained to supply the amount of sand required by the sedimentation model. We can evaluate the validity of this assumption for areas where the sand content was measured. The average sand content of near-surface sediments from western Mississippi Sound (Fig. 5A) is approximately 30%. The mud drape is estimated to be 0.05–0.1 m thick and, assuming no advection of sand or mud, the thickness of the total storm bed should be less than 0.15 m. The model predicts a Camille sand layer 0.15 m thick (Fig.

12A), which is three times that estimated from the cores; however, the model output is dominated by erosion from a nearby island (see Fig. 11B). The predicted sand bed from the 1947 hurricane is less than 0.01 m thick because of reduced coastal erosion and transport in this area.

The thickest sand layers are predicted near the barrier islands and within tidal passes. The most important source of sand is the shoreface, which is parameterized by the landward boundary condition in the model. Thus, the sand layer is almost 0.3 m at Ship Island and 0.2 m in Chandeleur Sound, which are both behind the barriers; however, amalgamation dominates at these locations. Sand is transported by the ebbing storm surge currents through the passes, producing thick, amalgamated beds as at Dog Keys Pass. Sediment deposited on the inner shelf is both locally resuspended and transported from the Gulf side of the barrier islands, producing irregular, discrete sand beds less than 0.2 m thick. Finally, thin, discrete sand beds are predicted in the most protected areas such as Lake Borgne, but bioturbation can rapidly destroy all primary fabric where storm deposition is reduced.

4.2. Amalgamation and bioturbation

Resuspension and erosion can rework existing deposits, thereby producing amalgamated beds and homogeneous ^{210}Pb profiles. In all locations with geochronological control, the Camille bed is preserved to some extent (sandy bed, vertical $^{210}Pb_{xs}$ profile with a base marked by the maximum penetration of ^{137}Cs), and the original bed thickness can be estimated from the core data. Radiometric and physical data at stations 5 and 6 suggest that the geologic signatures of both Hurricane Camille and the 1947 hurricane are preserved in western Mississippi Sound. This is supported by the simulated stratigraphy in Fig. 12. Furthermore, knowledge of the environmental forcing used in the model simulations shows that weaker waves and currents reduce resuspension and transport during storms. Reduced bioturbation in areas with lower salinity and reduced circulation, such as the western Mississippi Sound and Lake Borgne, is thus a major factor in preservation.

The simulated cores indicate that Camille may have reworked at least part of the 1947 storm bed in the eastern portion of the study area. The presence of only one bed in the simulated core at Ship Island (Fig. 10A) indicates that all of the 1947 sand layer was incorporated into the Camille bed. This is consistent with the homogeneous bedding (Fig. 4C) and gamma density profile (Fig. 6C) at station 2. Part of the older sand layer was amalgamated with the Camille bed at Dog Keys Pass (Fig. 10B) and within Chandeleur Sound (Fig. 13B). The resuspension depth is limited by the active layer thickness in the model (Keen and Glenn, 1998). Consequently, bed amalgamation predominantly occurs in areas where the storm currents are largest during the Hurricane Camille simulation. More specifically, when the suspended load transport gradient increases in the flow direction, erosion is predicted by the model; thus the removal of older sediment occurs near tidal passes where the flow accelerates and changes direction rapidly.

Bioturbation further modifies the storm beds, resulting in mottled fabric and truncated sand lenses as seen in X-radiographs (Fig. 4) and indicated in model simulations (Fig. 15). Only in cases where the bioturbation depth is less than the bed thickness has primary depositional bedding been preserved. It is also possible to preserve bedding in cases where individual beds are thinner than the bioturbation depth but where rapid burial occurs (e.g., Wheatcroft, 2000 and references therein). This is not the case for our study area, however, because sediment accumulation between 1947 and 1969 was relatively slow (approximately 0.002 m year^{-1}) and the time span between storms was sufficient to allow almost total bioturbation of the shallow seabed. Thus, bed preservation with respect to bioturbation is primarily controlled in this case by initial bed thickness, bioturbation rate, and bioturbation depth.

5. Conclusions

Two sandy layers have been identified in box cores and gravity cores from the Mississippi Sound area using radiometric, physical, and sedimentological methods. The older bed was deposited by an unnamed hurricane from 1947. Hurricane Camille made landfall in the area in 1969 and produced a second sandy layer that is observed in cores from the region. Sedimentary fabric within the cores varies from stratified to bioturbated.

The deposition of the original sandy storm beds has been simulated using a numerical sediment resuspension and transport model, which is forced by numerical wave and current models. The sedimentation model predicts a sandy bed that varies in thickness with distance from landfall. The thickest sand layers are deposited on the inner shelf near barrier islands and tidal passes, which act to focus and intensify the sediment-laden storm surge ebb flows. These deposits exceed 0.5 m for both storms. The simulated 1947 hurricane sand layer inside Chandeleur Sound is irregular near the storm track, with a maximum thickness of 0.4 m. This bed thins to less than 0.05 m within Mississippi Sound, which is 50 km from landfall. The simulated Hurricane Camille storm currents are stronger than the 1947 hurricane and thus a thicker bed is predicted. This bed exceeds 1 m inside Mississippi Sound near the barrier islands. The inner-shelf bed is also more widespread, extending from Mississippi Sound in the north to the modern Mississippi River delta, more than 100 km distant. Both hindcast storms produce a thin sand layer within Lake Borgne, which is protected from strong wave action. Resuspension produces a uniform sand layer ranging from 0.01 to 0.04 m in thickness whereas advection and deposition result in an irregular bed, which is then disrupted further by bioturbation. These processes would produce mottled and truncated bedding as observed in X-radiographs.

The long-term sediment accumulation rate is sensitive to local advection during the storm, which can lead to low estimates in sediment source areas and high estimates in sink areas. Physical and biological processes are very important to the post-depositional modification of a storm layer. Consequently, because of non-uniform resuspension, erosion, deposition, and post-depositional modification by physical and biological processes, the preserved storm bed is not uniform in composition, thickness, or fabric. Thus, ''layer cake'' stratigraphic analysis principles cannot be used to evaluate the sedimentological impact and record of large storms.

Acknowledgements

This research was supported by the Office of Naval Research (T.R. Keen by program element 0601153N, C.A. Blain by program element 0602435N, and ONR grant N00014-00-1-0768 to S.J. Bentley), the Naval Research Laboratory (core fund support for ship time, and grant N00173-00-1-G907 to S.J. Bentley), and the Naval Oceanographic Office. Modeling and data requirements in support of the Northern Gulf of Mexico Littoral Initiative project of the Naval Oceanographic Office motivated this study. The authors also wish to thank R.L. Beavers and an anonymous reviewer for their constructive comments, which contributed to improving this manuscript.

References

Aigner, T., Reineck, H.E., 1981. Proximality trends in modern storm sands from the Helgoland Bight and their implications for basin analysis. Senckenbergiana Maritima 14, 183–215.

Anonymous, 1969. Hurricane Camille—A Preliminary Report. U.S. Department of Commerce, ESSA, Weather Bureau, 58 pp.

Beavers, R.L., 1999. Storm sedimentation on the surf zone and inner continental shelf, Duck, North Carolina. PhD Thesis, Duke University, Durham, North Carolina. 118 pp.

Benninger, L.K., Aller, R.C., Cochran, J.K., Turekian, K.K., 1979. Effects of sediment mixing on the ^{210}Pb chronology and trace metal distribution in a Long Island Sound sediment core. Earth and Planetary Science Letters 43, 241–259.

Bentley, S.J., 1998. The emplacement and evolution of sedimentary fabric: physical and biological influences in three contrasting depositional environments. PhD dissertation, State University of New York at Stony Brook, Marine Sciences Research Center. 275 pp.

Bentley, S.J., Nittrouer, C.A., 1999. Physical and biological influences on the formation of sedimentary fabric in an oxygen-restricted depositional environment: Eckernförde Bay, southwestern Baltic Sea. Palaios 14, 585–600.

Bentley, S.J., Sheremet, A., 2003. A new model for the emplacement, bioturbation, and preservation of sedimentary strata. Geology 31 (8) 725–728.

Bentley, S.J., Furukawa, Y., Vaughan, W.C., 2000. Record of event sedimentation in Mississippi Sound. Transactions-Gulf Coast Association of Geological Societies, 715–723.

Bentley, S.J., Keen, T.R., Blain, C.A., Vaughan, W.C., 2002. The origin and preservation of a major hurricane bed in the northern Gulf of Mexico: Hurricane Camille, 1969. Marine Geology 186, 423–446.

Blain, C.A., 1997. Modeling methodologies for the prediction of hurricane storm surge. In: Saxena, N. (Ed.), Recent Advances in Marine Science and Technology, vol. 96. Pacon International, Honolulu, Hawaii, pp. 177–189.

Booij, N., Ris, R.C., Holthuijsen, L.H., 1999. A third generation wave model for coastal regions: 1. Model description and validation. Journal of Geophysical Research 104, 7649–7666.

Cochran, J.K., 1982. The oceanic chemistry of the U- and Th-series nuclides. In: Ivanovich, J.K., Harmon, J.K. (Eds.), Uranium

Series Disequilibrium: Applications to Environmental Problems. Clarendon Press, Oxford, pp. 384–430.

Cutshall, N.H., Larsen, I.L., Olsen, C.R., 1983. Direct analysis of ^{210}Pb in sediment samples: self absorption corrections. Nuclear Instruments and Methods 206, 1–20.

Dellapenna, T.M., Kuehl, S.A., Schaffner, L.C., 2000. Sea-bed mixing and particle residence times in biologically and physically dominated estuarine systems: A comparison of lower Chesapeake Bay and the York River subestuary. Estuarine, Coastal and Shelf Science 46, 777–795.

Dott, R.H., Bourgeois, J., 1982. Hummocky stratification: significance of its variable bedding sequences. Geological Society of America Bulletin 93, 663–680.

Driese, S.G., Fischer, M.W., Easthouse, K.A., Marks, G.T., Gogola, A.R., Schoner, A.E., 1991. Model for genesis of shoreface and shelf sandstone sequences, southern Appalachians: paleoenvironmental reconstruction of an Early Silurian shelf system. In: Swift, D.J.P., Oertel, G.F., Tillman, R.W., Thorne, J.A. (Eds.), Shelf Sand and Sandstone Bodies. Special Publication-International Association of Sedimentologists, vol. 14. Blackwell Scientific, Boston, MA, pp. 309–338.

Duke, W.L., 1985. Hummocky cross-stratification, tropical hurricanes, and intense winter storms. Sedimentology 32, 167–194.

Glenn, S.M., Grant, W.D., 1987. A suspended sediment correction for combined wave and current flows. Journal of Geophysical Research 92, 8244–8246.

Hayes, M.O., 1967. Hurricanes as geologic agents: Case studies of Hurricanes Carla, 1961, and Cindy, 1963. Report of Investigations No. 61. Bureau of Economic Geology, Texas University.

Kahn, J.H., Roberts, H.H., 1982. Variations in storm response along a microtidal transgressive barrier-island arc. Sedimentary Geology 33, 129–146.

Keen, T.R., Glenn, S.M., 1994. A coupled hydrodynamic-bottom boundary layer model of Ekman flow on stratified continental shelves. Journal of Physical Oceanography 24, 1732–1749.

Keen, T.R., Glenn, S.M., 1998. Resuspension and advection of sediment during Hurricane Andrew on the Louisiana continental shelf. Proceedings of the 5th International Conference on Estuarine and Coastal Modeling, pp. 481–494.

Keen, T.R., Slingerland, R.L., 1993a. A numerical study of sediment transport and event bed genesis during Tropical Storm Delia. Journal of Geophysical Research 98, 4775–4791.

Keen, T.R., Slingerland, R.L., 1993b. Four storm-event beds and the tropical cyclones that produced them: a numerical hindcast. Journal of Sedimentary Petrology 63, 218–232.

Leuttich, R.A.. Westerink, J.J., Scheffner, N.W., 1992. ADCIRC: An advanced three-dimensional circulation model for shelves, coasts, and estuaries. Report 1: Theory and methodology of ADCIRC-2DDI and ADCIRC-3DI. Technical report DRP-92-6, Dept. of the Army. 168 pp.

Ludwick, J.C., 1964. Sediments in northeastern Gulf of Mexico. In: Miller, R.L. (Ed.), Papers in Marine Geology: Shepard Commemorative Volume. MacMillan, New York, pp. 204–238.

Morton, R.A., 1981. Formation of storm deposits by wind-forced currents in the Gulf of Mexico and the North Sea. In: Nio, Shuttenhelm, R.T.E., vanWeering, Tj.C.E. (Ed.), Holocene Marine Sedimentation in the North Sea Basin. Special Publication-International Association of Sedimentologists, vol. 5, pp. 385–396.

Murray, S.P., 1970. Bottom currents near the coast during Hurricane Camille. Journal of Geophysical Research 75, 4579–4582.

Neumann, C.J., 1993. Tropical cyclones of the North Atlantic Ocean, 1871–1977. National Oceanic and Atmospheric Administration, Washington. 170 pp.

Nittrouer, C.A., Sternberg, R.W., 1981. The formation of sedimentary strata in an allochthonous shelf environment: The Washington continental shelf. Marine Geology 42, 201–232.

Nittrouer, C.A., DeMaster, D.J., McKee, B.A., Cutshall, N.H., Larsen, N.H., 1984. The sediment mixing on ^{210}Pb accumulation rates for the Washington continental shelf. Marine Geology 54, 201–221.

Nummedal, D., Penland, S., Gerdes, R., Schramm, W., Kahn, J., Roberts, H., 1980. Geologic response to hurricane impact on low-profile Gulf Coast barriers. Transactions-Gulf Coast Association of Geological Societies 30, 183–195.

Oey, L., Chen, P., 1992. A nested-grid ocean model: With application to the simulation of meanders and eddies in the Norwegian coastal current. Journal of Geophysical Research 97, 20063–20086.

Otvos, E.G., 1970. Development and migration of barrier islands, northern Gulf of Mexico. Geological Society of America Bulletin 81, 241–246.

Ris, R.C.., Holthuijsen, L.H., Booij, N., 1999. A third generation wave model for coastal regions: 2. Verification. Journal of Geophysical Research 104, 7667–7681.

Snedden, J.W., Nummedal, D., 1990. Coherence of surf zone and shelf current flow on the Texas (U.S.A.) coastal margin: implications for interpretation of paleo-current measurements in ancient coastal sequences. Sedimentary Geology 67, 221–236.

Snedden, J.W., Nummedal, D., 1991. Origin and geometry of storm-deposited sand beds in modern sediments of the Texas continental shelf. In: Swift, D.J.P., Oertel, G.F., Tillman, R.W., Thorne, J.A. (Eds.), Shelf Sand and Sandstone Bodies. Special Publication-International Association of Sedimentologists, vol. 14. Blackwell Scientific, Boston, MA, pp. 283–308.

Snedden, J.W., Nummedal, D., Amos, A.F., 1988. Storm- and fair-weather combined flow on the central Texas continental shelf. Journal of Sedimentary Petrology 58, 580–595.

Stone, G.W., Stapor, F.W., 1996. A nearshore sediment transport model for the northeast Gulf of Mexico coast. Journal of Coastal Research 12 (3), 786–792.

Stone, G.W., Wang, P., 1999. The importance of cyclogenesis on the short-term evolution of Gulf coast barriers. Transactions-Gulf Coast Association of Geological Societies XLIX, 47–48.

Stone, G.W., Grymes, J.W., Dingler, J.R., Pepper, D.A., 1997. Overview and significance of hurricanes on the Louisiana coast, USA. Journal of Coastal Research 134 (3), 656–669.

Stone, G.W., Wang, P., Pepper, D.A., Grymes, J.W., Roberts, H.H., Zhang, X.P., Hsu, S.A., Huh, O.K., 1999. Researchers begin to unravel the significance of Hurricanes of the northern Gulf of Mexico. EOS, Transactions of the American Geophysics Union.

Thorne, J.A., Grace, E., Swift, D.J.P., Niedoroda, A., 1991. Sedimentation on continental margins: III. The depositional fabric and analytical approach to stratification and facies identification.

In: Swift, D.J.P., Oertel, G.F., Tillman, R.W., Thorne, J.A. (Eds.), Shelf Sand and Sandstone Bodies. Special Publication-International Association of Sedimentologists, vol. 14. Blackwell Scientific, Boston, MA, pp. 59–88.

Upshaw, C.F., Creath, W.B., Brooks, F.L., 1966. Sediments and microfauna off the coasts of Mississippi and adjacent states. Bulletin-Mississippi Geological Survey 106. 127 pp.

Wheatcroft, R.A., 2000. Oceanic Flood Sedimentation: a new perspective. Continental Shelf Research 20, 2059–2066.